Chemical Geology xxx (2009) xxx–xxx

Contents lists available at ScienceDirect

Chemical Geology

journal homepage: www.elsevier.com/locate/chemgeo

Deglacial variations of Sr and $^{87}Sr/^{86}Sr$ ratio recorded by a stalagmite from Central China and their association with past climate and environment

Houyun Zhou [a,b,f,*], Yue-xing Feng [c], Jian-xin Zhao [c], Chuan-Chou Shen [d], Chen-Feng You [e], Yin Lin [d]

[a] School of Geography, South China Normal University, Guangzhou 510631, China
[b] State Key Laboratory of Loess and Quaternary Geology, Institute of Earth Environment, Chinese Academy of Sciences, Xi'an, 710075, China
[c] Radiogenic Isotope Laboratory, Centre for Microscopy and Microanalysis, the University of Queensland, Brisbane, Qld 4072, Australia
[d] Department of Geosciences, National Taiwan University, Taipei 106, Taiwan, ROC
[e] The Earth Dynamic System Research Center, National Cheng-Kung University, Tainan 701, Taiwan, ROC
[f] Guangzhou Institute of Geochemistry, Chinese Academy of Sciences, Guangzhou 510640, China

ARTICLE INFO

Article history:
Received 24 November 2008
Received in revised form 1 September 2009
Accepted 4 September 2009
Available online xxxx

Editor: B. Bourdon

Keywords:
Speleothem
Strontium
Strontium isotope ratio
The last deglaciation
Wind-blown dust
Central China

ABSTRACT

A low-resolution strontium isotopic ratio ($^{87}Sr/^{86}Sr$) record coupled with a high-resolution Sr concentration profile covering the last deglacial period were obtained for a stalagmite, SJ3, collected from Songjia Cave, northeast Sichuan province, Central China. Both Sr and $^{87}Sr/^{86}Sr$ display significant variations during the period between 20 and 10 ka, which correlate well with oxygen isotope records from Greenland ice cores and speleothems in the East Asian summer monsoon regime, with higher Sr and more radiogenic $^{87}Sr/^{86}Sr$ values occurring during cold-dry climatic phases and vice versa. The Sr in SJ3 shows a negative linear relationship between $^{87}Sr/^{86}Sr$ and 1/Sr, suggesting the binary mixing of two end-members, the host rock of Late Permian limestone with a relatively lower $^{87}Sr/^{86}Sr$ ratio (~0.7071) and an exotic Sr source with a relatively radiogenic $^{87}Sr/^{86}Sr$ ratio (~0.7109 deduced from the $^{87}Sr/^{86}Sr$-1/Sr correlation). Atmospheric dust activity was suggested to be the most probable factor influencing the two indices. Because the carbonate fraction in wind-blown dust is enriched in Sr and has a more radiogenic $^{87}Sr/^{86}Sr$ ratio, enhanced atmospheric dust activity under stronger Asian winter monsoon which is associated with cold-dry climate would lead to higher Sr concentrations and more radiogenic $^{87}Sr/^{86}Sr$ ratios in SJ3 and vice versa. This interpretation is supported by the general parallelism of the two Sr indices to winter monsoon proxy from East Asia such as the dust flux and quartz median diameter in Luochuan loess profile during the same period. This study suggests that the speleothem $^{87}Sr/^{86}Sr$ ratio and Sr concentration, especially the former in northeastern Sichuan Province can be used to investigate the atmospheric dust activity and Asian winter monsoon.

1. Introduction

In areas intensively influenced by the East Asian summer monsoon (EASM), speleothem-derived stable oxygen isotope ($\delta^{18}O$) records have been widely and successfully used to reconstruct summer monsoon intensity and amount of precipitation (Wang et al., 2001; Zhao et al., 2003; Yuan et al., 2004; Dykoski et al., 2005; Wang et al., 2008; Hu et al., 2008; Zhou et al., 2008a,b). Meanwhile, however, much less attention has been paid to other proxies such as annual layer thickness of stalagmite, trace elements and uranium and strontium isotopic compositions ($^{234}U/^{238}U$ and $^{87}Sr/^{86}Sr$) (e.g., Fairchild et al., 2006a). These proxies, especially trace elements such as magnesium (Mg), strontium (Sr) and barium (Ba) have been demonstrated to be appropriate and were often used for reconstruction of past climate and environment (Goede et al., 1998; Roberts et al., 1998, 1999; Fairchild et al., 2001; Huang et al., 2001; Baldini et al., 2002; Ma et al., 2003; Treble et al., 2003; Li et al., 2005a; Cruz et al., 2007). In the EASM regime, only a few attempts have been made to investigate past climate and environment using speleothem-derived trace element records (Ma et al., 2003; Hu et al., 2005; Li et al., 2005a; Johnson et al., 2006; Zhou et al., 2008c,d). For example, Li et al. (2005a) reported a long-term record of Sr/Ca ratio but with a relatively low resolution. The trace metal records reported by Johnson et al. (2006) had a high resolution but covered a very short period, less than 20 years, and thus cannot inform us how these trace metals behave during major climate shifts such as glacial–interglacial transition in the EASM regime.

In this paper, a high-resolution long-term Sr record is recovered from a stalagmite SJ3 collected from central China. This stalagmite was developed during the late Pleistocene from 38 to 10 ka and its stable isotopes ($\delta^{18}O$ and $\delta^{13}C$) and rare earth elements have been

* Corresponding author. Guangzhou Institute of Geochemistry, Chinese Academy of Sciences, No. 511, Kehua Street, Wushan, Tianhe, Guangzhou 510640, PR China. Tel.: +86 20 85290296; fax: +86 20 85290130.
E-mail address: hyzhou@gig.ac.cn (H. Zhou).

0009-2541/$ – see front matter © 2009 Elsevier B.V. All rights reserved.
doi:10.1016/j.chemgeo.2009.09.003

reported previously (Zhou et al., 2008a,c,d). For comparison, the Mg and Ba records for SJ3 are presented as well.

In addition to trace elements, $^{87}Sr/^{86}Sr$ data for SJ3 are also reported in this paper. Until now, only a few speleothem $^{87}Sr/^{86}Sr$ records have been reported (Banner et al., 1996; Goede et al., 1998; Ayalon et al., 1999; Bar-Matthews et al., 1999; Verheyden et al., 2000; Frumkin and Stein, 2004; Li et al., 2005a), which could be mainly due to the high cost for $^{87}Sr/^{86}Sr$ measurement. Speleothem $^{87}Sr/^{86}Sr$ ratio directly records the Sr isotopic composition of cave water and its variations reflect changes in relative contribution of various Sr sources that have different $^{87}Sr/^{86}Sr$ signatures (Faure and Mensing, 2005). One of the most important Sr sources for speleothem is the host rock (Banner et al., 1996; Goede et al., 1998; Ayalon et al., 1999; Bar-Matthews et al., 1999; Verheyden et al., 2000; Frumkin and Stein, 2004; Li et al., 2005a). Other significant sources include overlying soil layer, wind-blown dust and sea spray. In particular, previous studies suggested that speleothem $^{87}Sr/^{86}Sr$ variations might be related to atmospheric dust activity (Ayalon et al., 1999; Bar-Matthews et al.,

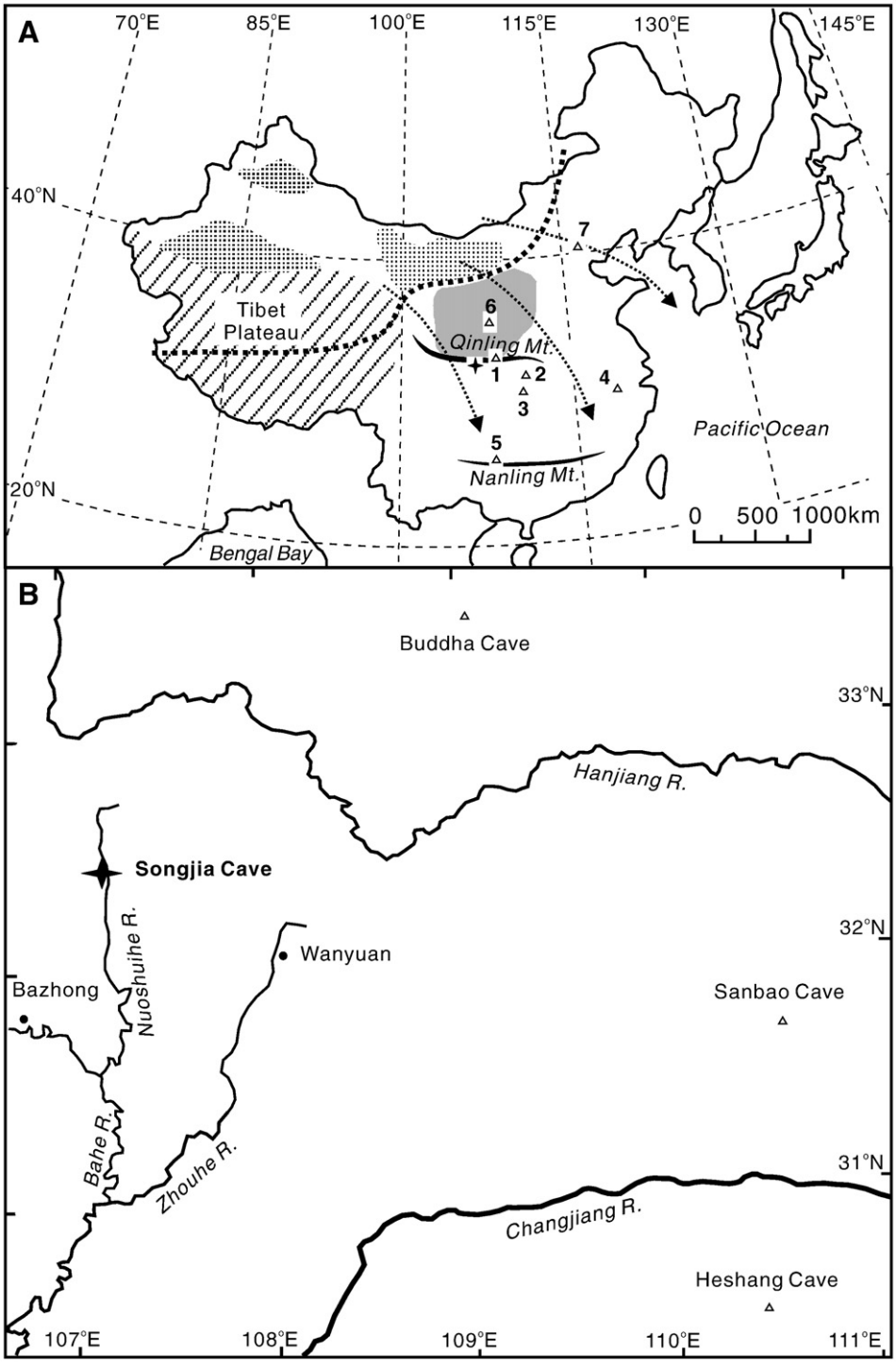

Fig. 1. Location of Songjia Cave [the star in (A)]. The cave is on the south flank of Qinling Mountain Ranges. In (A), the shaded area is the Loess Plateau; the dotted areas are deserts in northwest China; the hatched area is the Tibet Plateau; the thick dashed line indicates the northwestern limit of the East Asian summer monsoon; the dashed arrows indicate routes of winter monsoon and dust transportation. 1-Buddha Cave (Li et al., 2005a). 2-Sanbao Cave (Wang et al., 2008). 3-Heshang cave (Hu et al., 2005). 4-Hulu cave (Wang et al., 2001). 5-Dongge Cave (Yuan et al., 2004). 6-the Luochuan loess profile (Xiao et al., 1995). 7. Jingdong Cave in North China (Ma et al., 2003).

Please cite this article as: Zhou, H., et al., Deglacial variations of Sr and $^{87}Sr/^{86}Sr$ ratio recorded by a stalagmite from Central China and their association with past climate and environment, Chemical Geology (2009), doi:10.1016/j.chemgeo.2009.09.003

1999; Goede et al., 1998; Verheyden et al., 2000; Frumkin and Stein, 2004). Central China is on the main dust trajectory (Ginoux et al., 2001) and the Loess Plateau, which is a depocenter of wind-blown dust and deposits the thickest aeolian sediments in the world during Quaternary (Liu, 1985), is close to the study site (Fig. 1). Would the signal for past dust activity leave any imprint in speleothem $^{87}Sr/^{86}Sr$ record recovered from this area? This question arouses our interest in exploring the $^{87}Sr/^{86}Sr$ record of SJ3 and its paleoclimatic implications.

The main objectives for this study are (1) to investigate whether and how the speleothem-derived $^{87}Sr/^{86}Sr$ ratio and high-resolution Sr record are correlated with past climate and environment in the EASM regime during the great climate shift associated with the last deglaciation, and (2) to clarify whether Sr and $^{87}Sr/^{86}Sr$ bear information about past climate and environment that may not be revealed in speleothem $\delta^{18}O$ record, as the latter was related almost exclusively to the EASM strength and amount of associated precipitation (Wang et al., 2001; Zhao et al., 2003; Yuan et al., 2004; Dykoski et al., 2005; Wang et al., 2008; Zhou et al., 2008a,b). In particular, whether Sr and $^{87}Sr/^{86}Sr$ could provide information about dust activity which is associated with winter monsoon variations? If yes, the combination of trace elements, $^{87}Sr/^{86}Sr$, and the commonly used $\delta^{18}O$ and $\delta^{13}C$ would enable us to obtain a more comprehensive reconstruction of past climate and environment in the EASM regime.

2. Geological backgrounds and sample description

Stalagmite SJ3, 12.6-centimeter in length, was collected in 2004 from Songjia Cave in northeastern Sichuan Province, central China (107°10′45″E, 32°24′46″N) (Fig. 1). A detailed description of SJ3 and its geological backgrounds was given in Zhou et al. (2008a). In brief, Songjia cave, which is hosted in the Late Permian limestone (Bureau of Geology and Mineral Resources of Sichuan Province, 1991), is located in the south flank of the Qinling Mountain and is close to the Loess Plateau (Fig. 1). This site experiences a typical summer monsoon climate at present with an annual mean temperature of ~15 °C and an annual mean precipitation between 1000–1200 mm (Sinomaps Press, 1984). The highest temperature occurs during the summer season and most of the precipitation falls from May to October (Fig. 2). The site is also significantly influenced by the Asian winter monsoon at present and atmospheric dust activity is intensive during the winter season. Aeolian sediments are distributed sparsely in this area (Lei et al., 1998; Fang et al., 1999), suggesting that atmospheric dust activity was intensive as early as in Middle Pleistocene. Aeolian sediments are also the dominant source for local soil. The overlying soil layer on the limestone is usually less than 30 cm or absent in places. Local vegetation consists mainly of trees including pine, cypress and some deciduous broadleaf species.

On the exposed lengthwise cut surface of SJ3, a growth hiatus is apparent at depth of ~84 mm from its top (Fig. 3). Mg, Sr and Ba and $^{87}Sr/^{86}Sr$ ratio were determined for the part above the hiatus, corresponding to the time period from 20 to 10 ka. In general, the upper part of SJ3 (above the depth of ~40 mm) looks relatively pigmented compared with the section between the depths of 84 and 40 mm which seems to be relatively "clean" (Fig. 3). In particular, the top 6 mm of SJ3 is porous and rich in detrital materials (Zhou et al., 2008a), indicating several growth hiatuses (Figs. 3 and 4).

3. Methods

3.1. ^{230}Th dates and age model

Seven ^{230}Th dates previously reported (Zhou et al., 2008a) indicate that SJ3 developed between ~38 and ~10 ka and displays a nearly linear growth rate above the hiatus at 84 mm. Additional ^{230}Th dates, which were determined at the High-precision Mass Spectrometry and Environment Change Laboratory (HISPEC) of the National Taiwan University

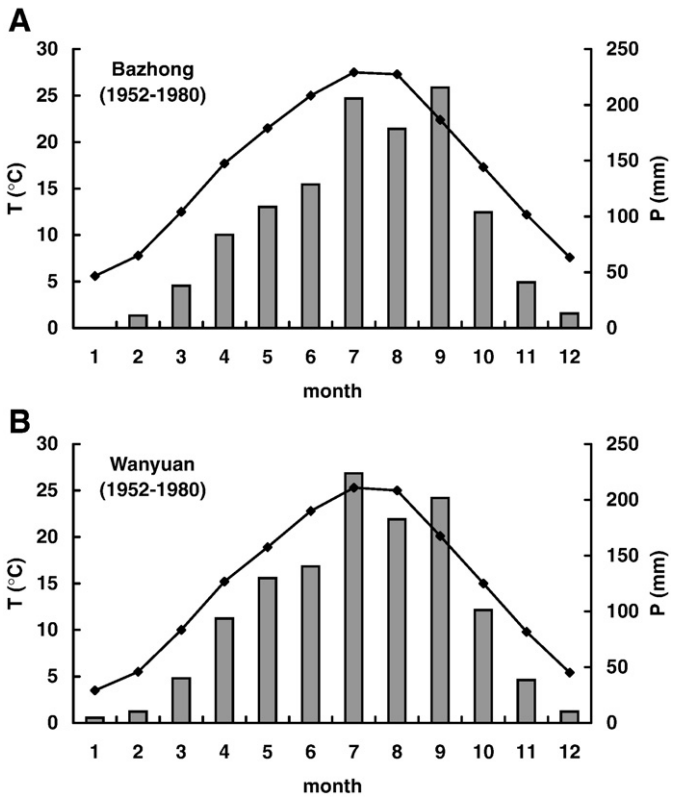

Fig. 2. Monthly mean temperature (T) (bars) and precipitation (P) (curves) at Bazhong (1952–1980) (A) and Wanyuan (1952–1980) (B), two meteorological stations closest to our study site (Fig. 1B). Data source: http://www.naturalresources.csdb.cn/newzrzy/gxzai1.asp.

(Shen et al., 2002; Frohlich et al., 2009) and the Radiogenic Isotope Laboratory of the University of Queensland (Table 1), however, indicate that the growth rate of SJ3 changes notably above the hiatus (Fig. 3). The dating method used in the University of Queensland was described in detail in Zhao et al. (2001) and Zhou et al. (2008b). As to the procedure used in the HISPEC, ^{238}U level was calculated from measurement of ^{235}U and the assumed natural $^{238}U/^{235}U$ atomic ratio of 137.88 with 2-sigma range of ±1‰ (e.g., Stirling et al., 2007; Weyer et al., 2008). The decay constants used are $9.1577\times10^{-6}yr^{-1}$ for ^{230}Th and $2.8263\times10^{-6}yr^{-1}$ for ^{234}U (Cheng et al., 2000), and $1.55125\times10^{-10}yr^{-1}$ for ^{238}U (Jaffey et al., 1971). Age corrections were calculated using an initial $^{230}Th/^{232}Th$ atomic ratio of 4±2 ppm; those are the values for a material at secular equilibrium with the crustal Th/U atomic ratio of 3.8 (Taylor and McLennan, 1985) with arbitrary uncertainty of 50%.

Analog to Zhou et al. (2008a), age model for SJ3 was established by linear interpolation according to depth between adjacent dated points except only for the layer at depth of 39 mm (Fig. 3). This is because the point at 39 mm has a ^{230}Th date precision of ±1.1 ka, 3–10 times worse than others due to a high ^{232}Th level, and displays a small reversion if the errors are not considered (Table 1). Although the growth rate of SJ3 may have changed during the period between 20 and 10 ka (Fig. 3), the similarity of the overall trend of the SJ3 $\delta^{18}O$ record to other speleothem $\delta^{18}O$ records from the EASM regime (Wang et al., 2001; Dykoski et al., 2005; Wang et al., 2008) and the Greenland ice core $\delta^{18}O$ record (Grootes et al., 1993; Stuiver et al., 1995) suggests that the age model is acceptable (Fig. 5). However, it must be emphasized that the age model for the 10–15 ka period has an age uncertainty of around ±500 years due to high levels of non-radiogenic ^{230}Th correction as reflected by high ^{232}Th (Table 1). In addition, the true age for the dirty porous section of the top 6 mm may not be reliable due to the unsuitability of material from this section for dating and obvious growth hiatuses in this section (see Zhou et al., 2008a; Fig. 4).

Please cite this article as: Zhou, H., et al., Deglacial variations of Sr and $^{87}Sr/^{86}Sr$ ratio recorded by a stalagmite from Central China and their association with past climate and environment, Chemical Geology (2009), doi:10.1016/j.chemgeo.2009.09.003

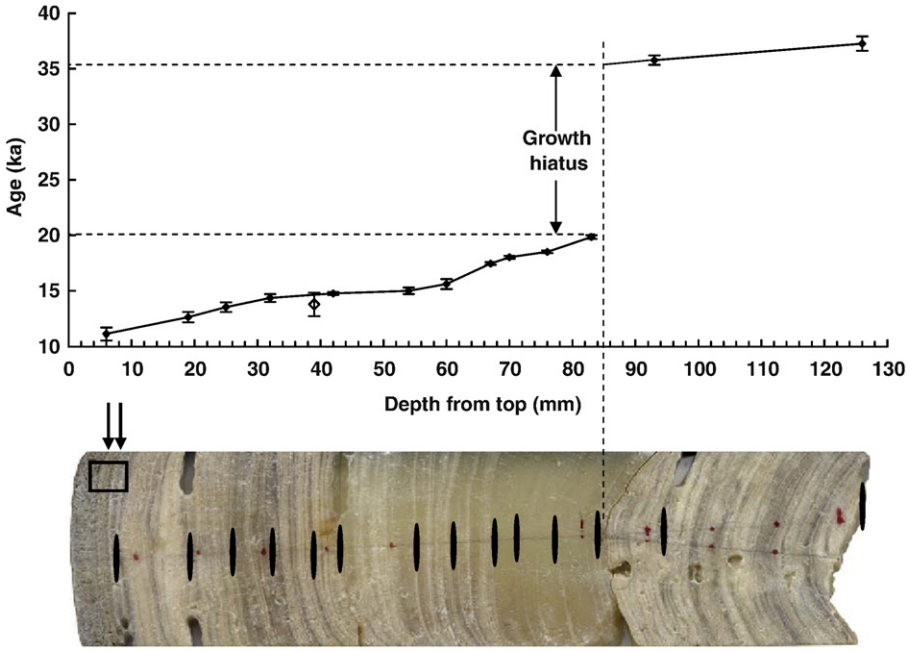

Fig. 3. Stalagmite SJ3 and its revised age model. Vertical bars indicate age error for each age determination. The vertical dashed line indicates the hiatus at 84 mm depth from top. On the image of SJ3, vertical black ellipses indicate the locations of ^{230}Th dates, the rectangle on the top indicate the location of Fig. 4. Arrows indicate locations of growth hiatuses in the dirty top of SJ3. Five previously reported ^{230}Th dates above the hiatus suggest a nearly linear correlation between date and depth (Zhou et al., 2008a). Additional ^{230}Th dates, however, indicate that the growth rate of SJ3 changes notably above the hiatus. The revised age model was established by linear interpolation between dated points according to depth from the top of SJ3 except the point at depth of 39 mm (see the text for explanation).

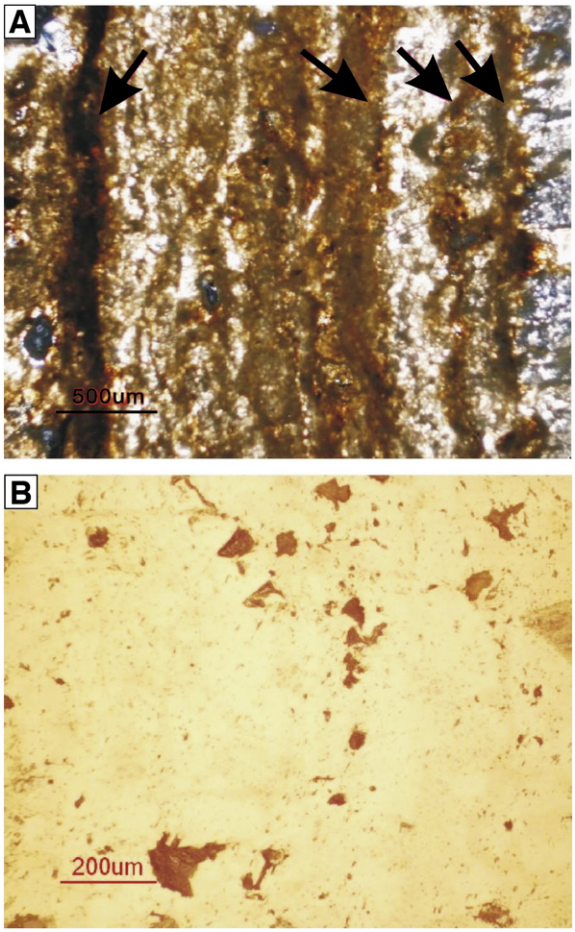

Fig. 4. Microscopic photos of the top dirt part of SJ3. The black arrows in (A) suggest several growth hiatuses and detrital materials are apparent in (B).

3.2. Sample collection

3.2.1. Sub-sampling of SJ3

Sub-samples from SJ3 for Mg, Sr and Ba measurement were obtained in the same way as those for δ^{18}O and δ^{13}C analysis (Zhou et al., 2008a), i.e. scraped with a scalpel along a thin slab previously taken along the central growth axis. The spatial resolution for Mg, Sr and Ba measurement is ~0.5 mm and a total of 168 sub-samples were analyzed with an average temporal resolution of ~60 years. Sub-samples for ^{87}Sr/^{86}Sr determination were also obtained along the central growth axis using a micro-drill with a spatial resolution of 2.5 mm. A total of 34 sub-samples were measured for ^{87}Sr/^{86}Sr ratios.

3.2.2. Sampling of the host rock, overlying soil layer, waters and cave sediments

In addition to stalagmite SJ3, the country rock hosting Songjia Cave, overlying soil layer and waters associated with Songjia Cave and cave sediments were also sampled. Three samples of the host rock of Late Permian limestone were collected with a hammer. Four soil samples were obtained from a soil profile above the cave, ~40 cm in depth and each represents a 10-cm interval. Three water samples were collected, including two pool water samples from Songjia Cave and a river water sample from the Nuoshuihe River which flows through the study area (Fig. 1). Water sample was firstly put into a big container (with a capacity of 5 L). After ~4 hours of particle settlement, ~500 ml of water was transferred into a bottle (with a capacity of 500 ml) and acidified to pH < 2 immediately with doubly distilled HNO_3 before the sample was transported to laboratory for geochemical analysis. Three cave sediment samples were collected on the floor in the cave using a shovel. These sediments were wet and loose and composed mostly of silicate materials. They would be leached by Milli-Q water to provide additional information on the Sr isotopic ratio of modern cave waters.

Please cite this article as: Zhou, H., et al., Deglacial variations of Sr and ^{87}Sr/^{86}Sr ratio recorded by a stalagmite from Central China and their association with past climate and environment, Chemical Geology (2009), doi:10.1016/j.chemgeo.2009.09.003

Table 1
U-series isotopic results and ages for stalagmite SJ3 from Songjia Cave.

Sample ID	Dist. from top mm	U ppm	±2σ	^{232}Th ppb	±2σ	^{230}Th/^{232}Th Atomic ratio, ppm	±2σ	^{230}Th/^{238}U Activity ratio	±2σ	^{234}U/^{238}U Activity ratio	±2σ	Uncorrected ^{230}Th age, ka	±2σ	Corrected ^{230}Th age, ka	±2σ	Corrected initial ^{234}U/^{238}U	±2σ
SJ3-006[a]	7	0.2705	0.0002	19.9	0.1	8.0		0.1947	0.0018	1.8044	0.0038	12.32	0.12	11.12	0.56	1.8471	0.0095
SJ3-019[b]	19	0.2856	0.0006	8.3	0.1	115.8	2.1	0.2039	0.0033	1.7963	0.0049	13.05	0.23	12.62	0.31	1.8252	0.0052
SJ3-025[b]	25	0.3272	0.0007	8.3	0.1	136.1	2.0	0.2093	0.0028	1.7360	0.0049	13.91	0.20	13.53	0.28	1.7647	0.0052
SJ3-032[a]	32	0.3928	0.0003	26.5	0.1	10.4		0.2316	0.0028	1.7865	0.0024	14.95	0.19	13.85	0.53	1.8332	0.0081
SJ3-032r[a]	32	0.3605	0.0003	23.7	0.1	11.3		0.2450	0.0016	1.7823	0.0021	15.91	0.11	14.84	0.49	1.8307	0.0078
SJ3-032c[c]	32													14.35	0.36		
SJ3-032t[b]	32	0.3640	0.0009	35.3	0.5	46.5	1.4	0.2730	0.0074	1.7755	0.0052	18.02	0.53	16.60	0.89	1.8127	0.0065
SJ3-039[b]	39	0.3310	0.0009	20.8	0.2	58.5	2.0	0.2230	0.0071	1.7548	0.0061	14.70	0.50	13.77	0.68	1.7847	0.0067
SJ3-042[a]	42	0.4014	0.0002	1.4	0.0	205.2		0.2275	0.0019	1.7709	0.0024	14.81	0.13	14.76	0.13	1.8046	0.0025
SJ3-054[b]	54	0.4206	0.0010	6.4	0.0	251.3	3.0	0.2324	0.0026	1.7697	0.0052	15.22	0.19	15.00	0.22	1.8030	0.0055
SJ3-060[b]	60	0.4472	0.0008	11.5	0.1	155.1	2.4	0.2426	0.0033	1.7644	0.0048	15.99	0.24	15.61	0.30	1.7988	0.0051
SJ3-067[a]	67	0.4583	0.0004	2.5	0.0	149.0		0.2706	0.0014	1.7971	0.0044	17.54	0.11	17.45	0.12	1.8388	0.0045
SJ3-070[a]	70	0.4261	0.0003	1.2	0.0	293.8		0.2770	0.0018	1.7898	0.0019	18.07	0.13	18.02	0.13	1.8319	0.0020
SJ3-076[b]	76	0.4444	0.0008	1.2	0.0	1707	12	0.2831	0.0014	1.7918	0.0042	18.55	0.11	18.51	0.11	1.8343	0.0045
SJ3-083[a]	83	0.3571	0.0005	3.1	0.0	103.7		0.2975	0.0019	1.7518	0.0038	19.98	0.15	19.83	0.16	1.7971	0.0040
SJ3-093[a]	93	0.2344	0.0002	9.1	0.1	38.8		0.4985	0.0040	1.7157	0.0035	36.42	0.35	35.77	0.43	1.8005	0.0056
SJ3-126[a]	126	0.2309	0.0001	23.2	0.1	16.2		0.5372	0.0024	1.7467	0.0018	38.89	0.21	37.26	0.65	1.8531	0.0116

[a] Ages determined at the University of Queensland. Ratios listed in the table refer to activity ratios normalized to the corresponding ratios measured for the HU-1 standard (See Zhou et al., 2008a).
[b] Ages determined at the National Taiwan University (Shen et al., 2002; Frohlich et al., 2009).
[c] A weighted mean age calculated using the data of SJ3-032 and SJ3-032r.

3.3. Analytical methods

Mg, Sr and Ba concentrations and $^{87}Sr/^{86}Sr$ ratios of SJ3 were obtained in the Radiogenic Isotope Laboratory, the University of Queensland. For trace element analysis, 3–5 mg of carbonate powder was dissolved in 2% nitric acid and diluted to between 1000 and 1200 times. Trace element measurement was performed on a Thermo X-series ICP-MS following the method of Eggins et al. (1997) with modifications as described in Li et al. (2005b) and ^{6}Li, ^{115}In, ^{187}Re, ^{209}Bi and ^{235}U were used as internal standards. $^{87}Sr/^{86}Sr$ measurement was conducted on a VG Sector-54 thermal ionization mass spectrometer (TIMS) after Sr was separated following standard cation exchange column procedures and standard SRM 987 was used for external calibration. The Sr blanks with the resin are less than 50 pg and at least four orders of magnitude lower than the sample Sr (>1000 ng). A SRM 987 standard was run after every ten samples were measured. Long-term repeated measurement of the SRM 987 standard on this machine yields a mean $^{87}Sr/^{86}Sr$ value of 0.710250 ± 0.000032 (2σ).

Soil samples were firstly crushed and gently ground. Then ~5 g of soil powder was put into a 50 ml centrifuge tube and about 25 ml of Milli-Q water was added to extract soluble metals in the soils (Liu et al., 2002a). After mixing evenly, the soil samples were ultrasonicated for 10 min at room temperature, centrifuged and the decanted solution was transferred into another pre-cleaned tube. Then 1% acetic acid was used to release carbonate-bounded elements as was adopted in leaching of loess and lacustrine sediments (Haskell et al., 1996; Yang et al., 2000; Liu et al., 2002a). It was added by once ~1 ml until complete reaction of carbonates. Totally ~5.5 g of 1% acetic acid was added and was mixed evenly with the residue. After 15 min further ultrasonication at room temperature, the mixture was centrifuged and the decanted solution was transferred into a third tube. The solutions leached consecutively with Milli-Q water and 1% acetic acid were measured for trace elements and $^{87}Sr/^{86}Sr$ ratio at the Earth Dynamic System Research Center (EDSRC) of the National Cheng-Kung University (NCKU). Trace elements were analyzed using a SF-ICP-MS (Element 2, Thermo Fisher Scientific) equipped with dual-type quartz spray chamber and micro-concentric PFA nebulizer (100 μm, ESI) as sample introduction system. $^{87}Sr/^{86}Sr$ ratios were determined on a Finnigan Triton TIMS after Sr was separated. The procedural blank of Sr is estimated to be ~300 pg, negligible compared with the amount of Sr analyzed which is usually greater than 600 ng. Reference material SRM 987 was used for quality control and a standard was run after every ten samples were measured. The long term reproducibility for SRM 987 on this machine is 0.710276 ± 0.000010 (2σ).

Cave water and river water and host rock samples were measured for Ca, Mg, Sr and Ba with a Varian Vista-PRO ICP-AES at Guangzhou Institute of Geochemistry. Water samples were 10–15 times pre-concentrated on hotplate before analysis. Preparation of cave sediments is similar to that of soil samples, but cave sediments were leached only with Milli-Q water and analyzed only for $^{87}Sr/^{86}Sr$ ratio. The $^{87}Sr/^{86}Sr$ ratios of these leachates and the water and rock samples were also measured at the EDSRC of NCKU.

4. Results

4.1. Sr and other elements

The Sr concentration of SJ3 is illustrated in Fig. 6a. It generally ranges from 100 to 260 ppm with an average of ~186 ppm and displays significant centennial variations with the highest concentration of ~290 ppm occurring at depth of ~48 mm and the lowest value of ~100 ppm at depth of ~7.5 mm from the top (Fig. 6a). With an overall decreasing trend from 84 to ~7 mm in depth, the Sr concentration of SJ3 shows clear increase from ~65 to 40 mm in

Please cite this article as: Zhou, H., et al., Deglacial variations of Sr and $^{87}Sr/^{86}Sr$ ratio recorded by a stalagmite from Central China and their association with past climate and environment, Chemical Geology (2009), doi:10.1016/j.chemgeo.2009.09.003

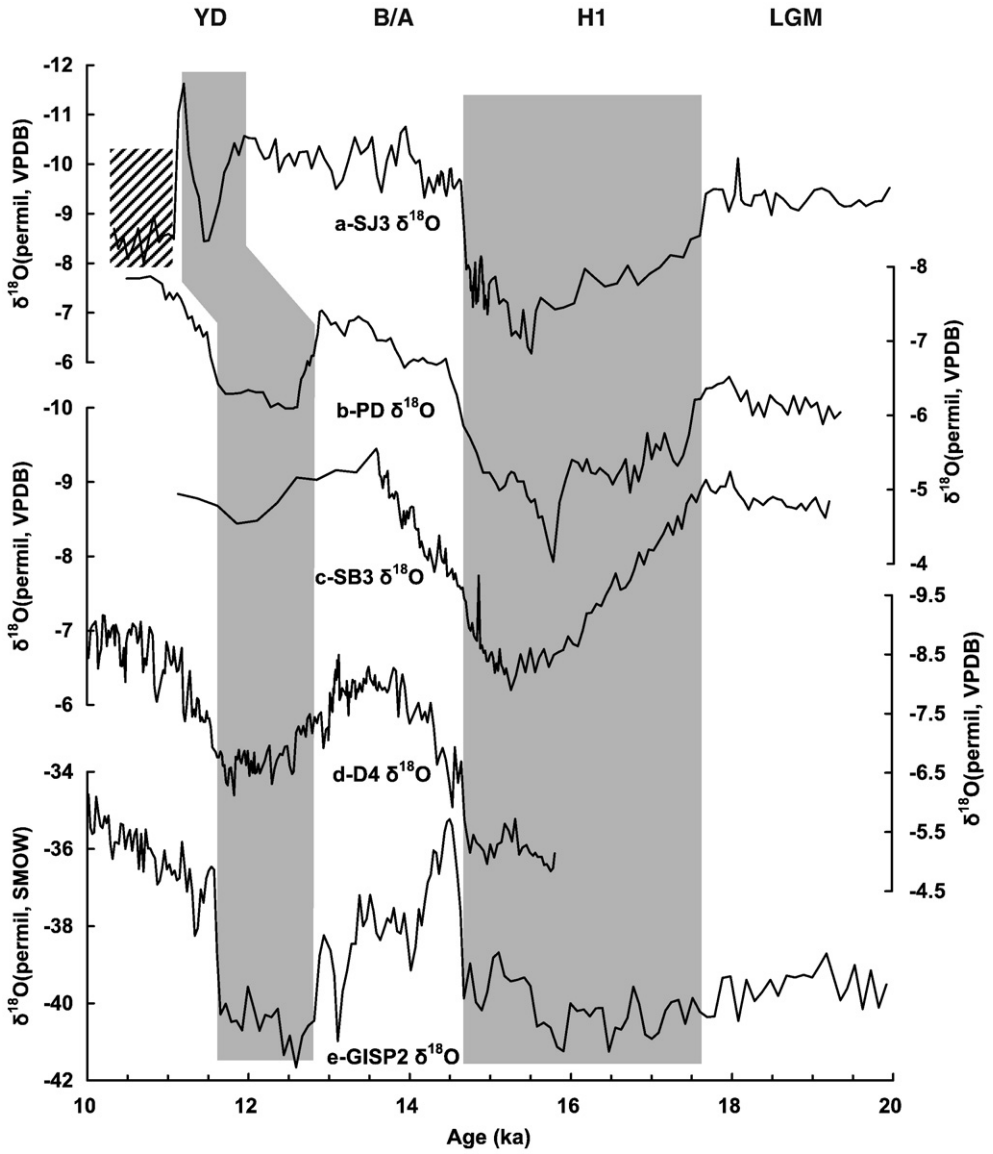

Fig. 5. Comparison of the $\delta^{18}O$ records between SJ3 and other speleothem archives in the EASM regime and polar ice core from Northern high latitude. (a) The SJ3 $\delta^{18}O$ record scaled with the age model revised in Fig. 3. (b) The PD $\delta^{18}O$ record from Hulu Cave in East China (Wang et al., 2001). (c) The SB3 $\delta^{18}O$ record from Sanbao Cave in Central China (Wang et al., 2008). (d) The D4 $\delta^{18}O$ record from Dongge Cave in Southwest China (Yuan et al., 2004). (e) The GISP2 ice core $\delta^{18}O$ record from Greenland (Grootes et al., 1993; Stuiver et al., 1995). The gray areas indicate two cold-dry phases associated with the Heinrich event 1 (H1) and Young Dyras (YD). The hatched area indicates the top part of SJ3 that might not precipitate under isotopic equilibrium (Zhou et al., 2008a). It is worthwhile to note that the SJ3 chronology for the period of 10–15 ka has a 2-sigma uncertainty of ~500 years. See Fig. 1 for locations of the caves in the EASM regime mentioned in text.

depth (Fig. 6a). For the top dirty part of SJ3, the Sr concentration shows a remarkable increase from ~110 ppm to ~200 ppm (Fig. 6a). Mg in SJ3 ranges from ~3200 to 9200 ppm and averages ~4900 ppm (Fig. 6b) while Ba in SJ3 ranges from 24 to 80 ppm and averages ~37 ppm (Fig. 6c). The general trend of Ba is parallel to the Sr record, but both are notably different from the Mg record (Figs. 6a–c and 7).

Ca in the three water samples ranges from 31.6 to 48.7 ppm, while the ranges for Mg, Sr and Ba are 6.9–11.0 ppm, 91.9–110 ppb and 11.1–23.8 ppb, respectively (Table 2). Also listed in Table 2 are the ratios of Mg/Ca, Sr/Ca and Ba/Ca for the host rock.

Ca, Mg, Sr, Ba, Al, Na, Mn and B leached consecutively from the soil samples by Milli-Q water and 1% acetic acid are listed in Table 3. It is clear that more Ca and Mg were leached out, either by Milli-Q water or by 1% acetic acid, compared to those reported in Li et al. (2005a). This may be due to difference in geological background and/or climate of the two sites. For example, the overlying soil layer and related loess deposits are 6–8 m thick at Zhen'an (Li et al., 2005a), but usually <30 cm at Songjia cave; annual precipitation at the study site is 1000 to 1200 mm (Fig. 2), much higher than ~560 mm at Zhen'an (Li et al., 2005a). The Ca, Mg, Sr and Ba leached out by 1% acetic acid are several times higher than those by Milli-Q water. This is consistent with the report by Liu et al. (2002a). Mg, Sr and Ba seem to be more easily leached by 1% acetic acid compared with Ca, leading to relatively higher Sr/Ca, Mg/Ca and Ba/Ca ratios in the 1% acetic acid leachate. Ca, Mg and Sr leached by 1% acetic acid from the lowest soil sample SJ-SI-Soil-4 are remarkably higher than leached from the above three soil samples (Table 3), which may be due to incorporation of small grains of limestone bedrock.

4.2. $^{87}Sr/^{86}Sr$ ratios

As illustrated in Fig. 6d, the $^{87}Sr/^{86}Sr$ ratios of SJ3 fall between 0.7085 and 0.7102 and average 0.7099. The highest $^{87}Sr/^{86}Sr$ ratio occurred at depth of 40 mm and the lowest at 2.5 mm. The top three $^{87}Sr/^{86}Sr$ ratios, which are from the top 6 mm porous and dirty part of uncertainty age (see Zhou et al., 2008a), are remarkably lower than

Please cite this article as: Zhou, H., et al., Deglacial variations of Sr and $^{87}Sr/^{86}Sr$ ratio recorded by a stalagmite from Central China and their association with past climate and environment, Chemical Geology (2009), doi:10.1016/j.chemgeo.2009.09.003

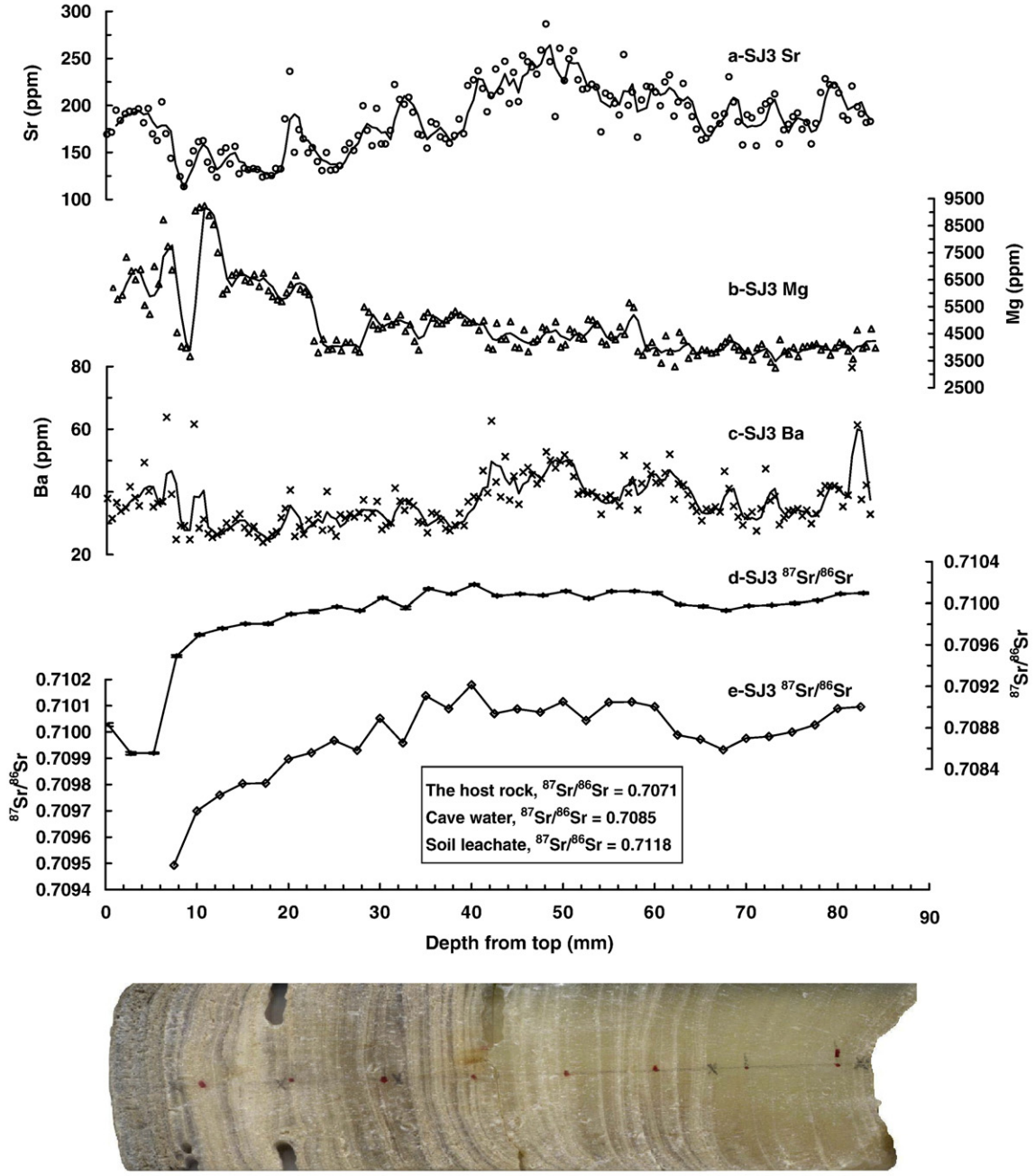

Fig. 6. The Sr (a), Mg (b), Ba (c) and $^{87}Sr/^{86}Sr$ ratio (d–e) records of SJ3. The solid line in (a), (b) and (c) represents a five-point running average trend of the data. Panel (e) is an enlargement of (d) for clarity. The values of average $^{87}Sr/^{86}Sr$ ratio of the host rock, cave water and soil leachate (by Milli-Q water) are shown on panel (e) for comparison.

the rest ratios; however, the remaining $^{87}Sr/^{86}Sr$ values still display significant variation (Fig. 6d). The $^{87}Sr/^{86}Sr$ ratio started with a decreasing trend from 0.7101 at depth of 82.5 mm to 0.7099 at 67.5 mm. Then it increased slightly until it reached a plateau of around 0.7101 at 60 mm. The plateau continued to the depth of 35 mm, and thereafter, the $^{87}Sr/^{86}Sr$ ratio decreased quickly and reached a value of 0.7095 at depth of 7.5 mm.

The $^{87}Sr/^{86}Sr$ data of the host rock, the cave and river waters, and leachates from overlying soil layer (leached by Milli-Q water and 1% acetic acid) and cave sediments (leached by Milli-Q water) are listed in Table 4. The $^{87}Sr/^{86}Sr$ ratios of the host rock have a narrow range from 0.7070 to 0.7072 and average ~0.7071, in line with the low $^{87}Sr/^{86}Sr$ ratio of seawater during the Late Permian (Burke et al., 1982; Hodell, 1994). The $^{87}Sr/^{86}Sr$ ratios of the leachates from soil samples fall between 0.7115 and 0.7121 with an average of 0.7118, consistent with the top $^{87}Sr/^{86}Sr$ ratio of carbonates from the Heimugou section at Luochuan in the Loess Plateau (Yang et al., 2000). In particular, for three of the four overlying soil samples, leachates by Milli-Q water have a little higher $^{87}Sr/^{86}Sr$ ratio than the subsequent leachates by 1% acetic acid. Two cave waters have $^{87}Sr/^{86}Sr$ ratios of 0.7084 and 0.7087, respectively, which are between the $^{87}Sr/^{86}Sr$ ratios of the host rock and the leachates from the overlying soil layer, suggesting that the Sr in cave water may be a mixture of Sr from the two sources. River water has a higher $^{87}Sr/^{86}Sr$ ratio than the cave waters have, implying Sr contributions from multiple, predominantly more radiogenic Sr source(s) in the catchment. Leachates from cave sediments are a little more radiogenic than cave waters (Table 4).

Please cite this article as: Zhou, H., et al., Deglacial variations of Sr and $^{87}Sr/^{86}Sr$ ratio recorded by a stalagmite from Central China and their association with past climate and environment, Chemical Geology (2009), doi:10.1016/j.chemgeo.2009.09.003

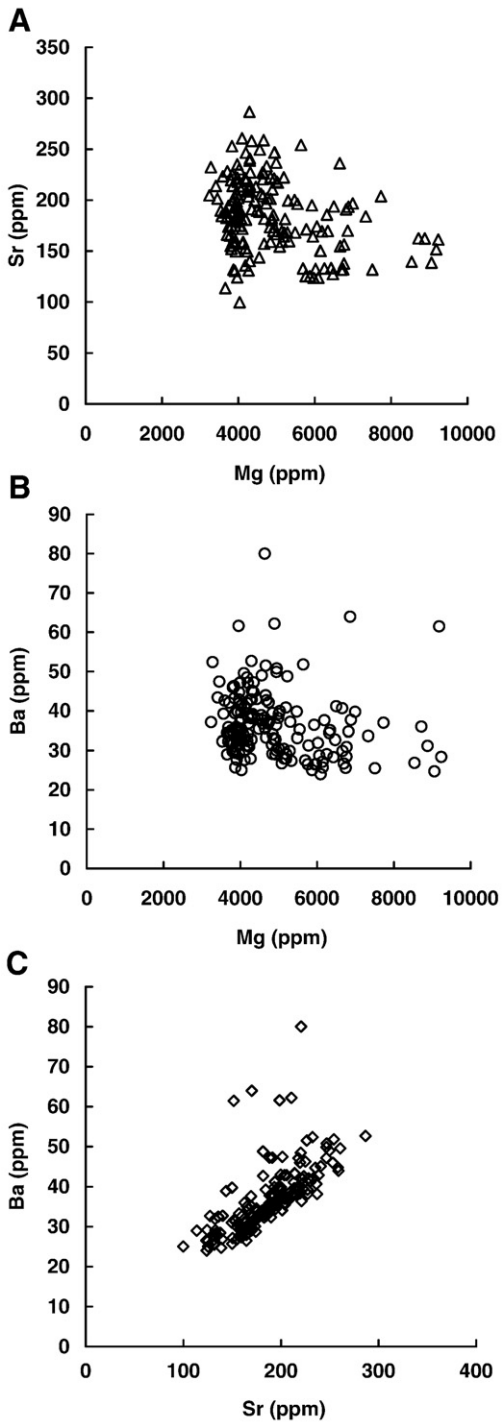

Fig. 7. Correlations among Mg, Sr and Ba of SJ3 for the period between 20 and 10 ka. (A) Sr–Mg; (B) Ba–Mg; (C) Ba–Sr.

5. Discussion

5.1. Association of Sr and $^{87}Sr/^{86}Sr$ ratio with past climate

Whether and how the significant variations of SJ3 Sr concentrations and $^{87}Sr/^{86}Sr$ ratios (Fig. 6a, d–e) are associated with changes in past climate and environment as is found in previous investigations (Banner et al., 1996; Goede et al., 1998; Ayalon et al., 1999; Bar-Matthews et al., 1999; Verheyden et al., 2000; Ma et al., 2003; Frumkin and Stein, 2004; Li et al., 2005a)? In Fig. 8 we compare the Sr concentrations and $^{87}Sr/^{86}Sr$ ratios of SJ3 with $\delta^{18}O$ records from the same stalagmite (Zhou et al., 2008a) and stalagmite PD from Hulu Cave in East China (Wang et al., 2001), and the Greenland ice core GISP2 (Grootes et al., 1993; Stuiver et al., 1995). The Mg and Ba records for SJ3 are also shown for comparison. The general trends of four curves, including the Sr concentrations and $^{87}Sr/^{86}Sr$ ratios of SJ3 and two speleothem $\delta^{18}O$ records, are similar, suggesting that the two Sr proxies are probably climatically related. Both Sr and $^{87}Sr/^{86}Sr$ display peak values during the coldest climatic phase of H1 and decreased notably after the transition to the Bϕlling–Allerϕd (B/A) warm period. It may be noted that during the top part of SJ3 the Sr concentration increases significantly from ~110 ppm to ~200 ppm (Figs. 6a and 8c), while the $^{87}Sr/^{86}Sr$ ratio displays an opposite trend, decreasing significantly from ~0.7095 to 0.7086. As suggested in another paper (Zhou et al., 2008a), this part may not have been deposited under isotopic equilibrium condition. Several growth hiatuses and obvious detrital grains (Fig. 4) indicate that this part of SJ3 may have developed after the flow path for SJ3 was changed and when SJ3 was occasionally fed by dripwater during rainfall extremes (Zhou et al., 2008a). The duration of the growth hiatuses in the top ~6 mm (Fig. 4) is unknown and it is unclear whether this top section grew in the early Holocene or much more recently, when the hydrology had significantly changed. Two $^{87}Sr/^{86}Sr$ ratios at depths of 2.5 and 5.0 mm may be obtained on growth hiatuses. Multi-proxies including $\delta^{18}O$ and $\delta^{13}C$ (Zhou et al., 2008a), trace elements such as Sr, Mg, Ba (Fig. 8) and petrographic structure (Fig. 4) imply that precipitation of calcite in this part may be caused mainly by evaporation between individual intensive percolations of groundwater resulted from rainfall extremes, leading to a significant increase in the concentration of Sr, Mg and Ba (Figs. 6 and 8) and a remarkable positive shift of $\delta^{18}O$ and $\delta^{13}C$ (see Fig. 4 in Zhou et al., 2008a). Associated decrease of 1/Sr due to evaporation may also be responsible for the excursion of the two $^{87}Sr/^{86}Sr$ ratios at depths of 2.5 and 5.0 mm from the negative linear $^{87}Sr/^{86}Sr$-1/Sr correlation as indicated in Fig. 7.

The Ba record displays a trend somehow parallel to the Sr record (Figs. 6 and 8). This parallelism was also revealed by some previous studies (Ayalon et al., 1999; Finch et al., 2001; Hellstrom and McCulloch, 2000; Roberts et al., 1998). Unlike Ba, Mg in SJ3 displays a trend very different from Sr (Figs. 6 and 8). A striking character of the Mg record is that it does not show any evident imprint of the H1 cold phase (Fig. 8g), which is well expressed in the $\delta^{18}O$ and $\delta^{13}C$ records (Zhou et al., 2008a) and the Sr concentrations and $^{87}Sr/^{86}Sr$ ratios (Fig. 8) of the same stalagmite, as well as in other climatic

Table 2
Ca, Mg, Sr and Ba in water samples (including cave water and river water) and host rock samples associated with Songjia Cave.

Sample ID	Locus	Sample type	Ca (ppm)	Mg (ppm)	Sr (ppb)	Ba (ppb)	Sr/Ca ($\times10^{-3}$)	Mg/Ca	Ba/Ca ($\times10^{-3}$)
SJDO	Songjia Cave	Pool water	48.7	11.0	91.9	15.4	1.89	0.226	0.316
SJDE	Songjia Cave	Pool water	37.1	9.4	110	11.1	2.98	0.253	0.299
RW	Nuoshuihe River	River water	31.6	6.9	108	23.8	3.40	0.218	0.753
LF-SZ-R		Limestone					0.808	0.015	0.003
SZ-R-in		Limestone					0.824	0.008	0.002
SI-SJ-R		Limestone					1.14	0.012	0.003

Please cite this article as: Zhou, H., et al., Deglacial variations of Sr and $^{87}Sr/^{86}Sr$ ratio recorded by a stalagmite from Central China and their association with past climate and environment, Chemical Geology (2009), doi:10.1016/j.chemgeo.2009.09.003

Table 3
Trace elements in the overlying soil layer leached sequentially with Milli-Q water and 1% acetic acid.

Sample ID	Depth (cm)	Leachate with Milli-Q water										
		Ca (ppm)	Mg (ppm)	Sr (ppb)	Ba (ppb)	Al (ppb)	Mn (ppb)	Na (ppb)	B (ppb)	Sr/Ca ($\times10^{-3}$)	Mg/Ca	Ba/Ca ($\times10^{-3}$)
SJ-SI-Soil-1	0–10	132	19.8	62.7	46.4	825	4.74	89.4	48.9	0.475	0.150	0.352
SJ-SI-Soil-2	10–20	153	19.6	65.9	48.8	422	4.00	95.9	85.4	0.431	0.128	0.319
SJ-SI-Soil-3	20–30	99.4	12.0	41.4	33.5	752	4.16	93.5	23.5	0.416	0.121	0.337
SJ-SI-Soil-4	30–40	194	18.9	74.6	42.9	292	3.66	111.3	14.0	0.385	0.097	0.221
Sample ID		Leachate with 1% acetic acid										
		Ca (ppm)	Mg (ppm)	Sr (ppb)	Ba (ppb)	Al (ppb)	Mn (ppb)	Na (ppb)	B (ppb)	Sr/Ca ($\times10^{-3}$)	Mg/Ca	Ba/Ca ($\times10^{-3}$)
SJ-SI-Soil-1		460	80.6	332	529	531	923	38.6	43.4	0.722	0.175	1.15
SJ-SI-Soil-2		508	80.8	323	520	630	1895	42.4	36.8	0.636	0.159	1.02
SJ-SI-Soil-3		491	66.2	314	512	619	4199	50.8	25.4	0.640	0.135	1.04
SJ-SI-Soil-4		1696	116	552	485	25.8	178	41.9	8.99	0.325	0.068	0.286

Concentration of trace element was reported relative to bulk dry soil sample.

proxies from East Asia (Ren et al., 1996; Wang et al., 2001; Dykoski et al., 2005). Like Sr, both Ba and Mg show a significant increase in the top dirty section of SJ3 (Figs. 6 and 8f–g), which may be due to aforementioned evaporation of dripwater between individual intensive percolations of groundwater.

In the study of stalagmite SFL from Buddha Cave at Zhen'an in southern Shanxi Province, Central China (about 200 km northeast of Songjia Cave, Fig. 1), Li et al. (2005a) found that most of the Sr in SFL came from the overlying soil layer and that higher $^{87}Sr/^{86}Sr$ ratios occurred under relatively warm-humid climate. They suggested that $^{87}Sr/^{86}Sr$ ratios were dominated by Sr released in chemical weathering of the soil and that increasing chemical weathering of the soil under relatively warm-humid climate was responsible for the relatively higher $^{87}Sr/^{86}Sr$ ratios in SFL. The association of speleothem $^{87}Sr/^{86}Sr$ ratio with climatic phase recorded in SJ3, with higher $^{87}Sr/^{86}Sr$ ratio corresponding to colder and drier climate (Fig. 8), is opposite to what documented in SFL (see Fig. 7 in Li et al., 2005a). This may be due to aforementioned differences in their local soil layers and climates (see Section 4.1). Weathering profile (with more radiogenic ^{87}Sr) might have made a much higher Sr contribution to stalagmite SFL than to SJ3. In addition, leaching of the overlying soil layer by precipitation should be more effective at the study site than at Zhen'an and variation of Sr supply directly from atmospheric dust activity should be more sensitively recorded in the $^{87}Sr/^{86}Sr$ ratio of SJ3.

The Young Dryas (YD) cold reversal was not evident in the $^{87}Sr/^{86}Sr$ variations (Fig. 8d). This may be due to insufficient sampling resolution and a much larger uncertainty in our U/Th dates for the YD period, or alternatively a different mechanism operating during the YD period. In the Western Pacific and East Asia, whether the YD cooling event has been ubiquitously registered is still in debate (see literature reviewed in Zhou et al., 2007). The Sr record, however, seems to show a weak YD signal where a YD-like event was previously suggested by Zhou et al. (2008a) (Fig. 8c). A detailed comparison between the SJ3 Sr record and the GISP2 $\delta^{18}O$ record (Grootes et al., 1993; Stuiver et al., 1995) indicates that five centennial cold events during the B/A warm period and the YD cold reversal in the polar region seem to correlate well with the Sr record within age errors (Fig. 8b–c).

Table 4
$^{87}Sr/^{86}Sr$ ratios of the Late Permian limestone, leachates of the overlying soil layer and cave sediments, river water and cave waters.

Sample ID	Sample Type	$^{87}Sr/^{86}Sr$	Within-run error ($2\sigma_m$, $\times10^{-6}$)
LF-SZ-R	Limestone	0.707127	8
SZ-R-in	Limestone	0.707000	9
SI-SJ-R	Limestone	0.707212	12
Average		0.707113	
RW	River water	0.709580	8
SJDE	Cave water	0.708428	7
SJDO	Cave water	0.708661	11
average		0.708545	
SJ-en-in	Cave sediments	0.709005	46
SJ-en-out	Cave sediments	0.708931	27
SJ-en-outc	Cave sediments	0.708857	31
Average		0.708931	
SJ-SI-soil-1	Soil	0.711562	7
		(0.711528)	(7)
SJ-SI-soil-2	Soil	0.711666	13
		(0.711670)	(6)
SJ-SI-soil-3	Soil	0.712080	10
		(0.711949)	(7)
SJ-SI-soil-4	Soil	0.712019	11
		(0.711887)	(7)
average		0.711832	
		(0.711759)	

Note: (1) The long term reproducibility for standard NBS 987 on the TIMS at EDSRC of NCKU is 0.710276 ± 0.000010 (2σ). (2) The data in parentheses represent solution leached by 1% acetic acid, while the others represent solution leached by Milli-Q water.

5.2. Sources of Sr

Possible sources for Sr in speleothems include the host rock, the overlying soil layer and some other potential sources such as atmospheric dust and sea spray (Nakano et al., 1993; Banner et al., 1996; Goede et al., 1998; Ayalon et al., 1999; Bar-Matthews et al., 1999; Verheyden et al., 2000; Frumkin and Stein, 2004; Richter et al., 2004; Hu et al., 2005; Li et al., 2005a). At the study site, Sr contribution from sea spray should be negligible because Songjia Cave is far away from coastline (>1000 km, Fig. 1); whereas atmospheric dust activity is intensive during the winter season. As at nearby Zhen'an, aeolian sediments are the sources for the overlying soil layer (Li et al, 2005a). Thus Sr in SJ3 can be regarded to come from two sources, the host rock (Late Permian limestone) and wind-blown dust, the latter being abundant in the Qinling Mountain since the Middle Pleistocene (Lei et al., 1998; Fang et al., 1999) and its carbonate fraction having much higher Sr concentration (>1000 ppm) and more radiogenic $^{87}Sr/^{86}Sr$ ratio (~0.710) compared with the host rock (Gallet et al., 1996; Yang et al., 2000; Jahn et al., 2001; Table 4). This is supported by the $^{87}Sr/^{86}Sr$ ratios of SJ3 which fall between the host rock and the leachates of the overlying soil layer (Table 4).

The aeolian sediments in central China are composed mostly of silicate minerals but also contain some carbonates (Wen et al., 1989; Gallet et al., 1996; Yang et al., 2000; Jahn et al., 2001). The carbonate fraction is more removable under natural weathering than the silicate

Please cite this article as: Zhou, H., et al., Deglacial variations of Sr and $^{87}Sr/^{86}Sr$ ratio recorded by a stalagmite from Central China and their association with past climate and environment, Chemical Geology (2009), doi:10.1016/j.chemgeo.2009.09.003

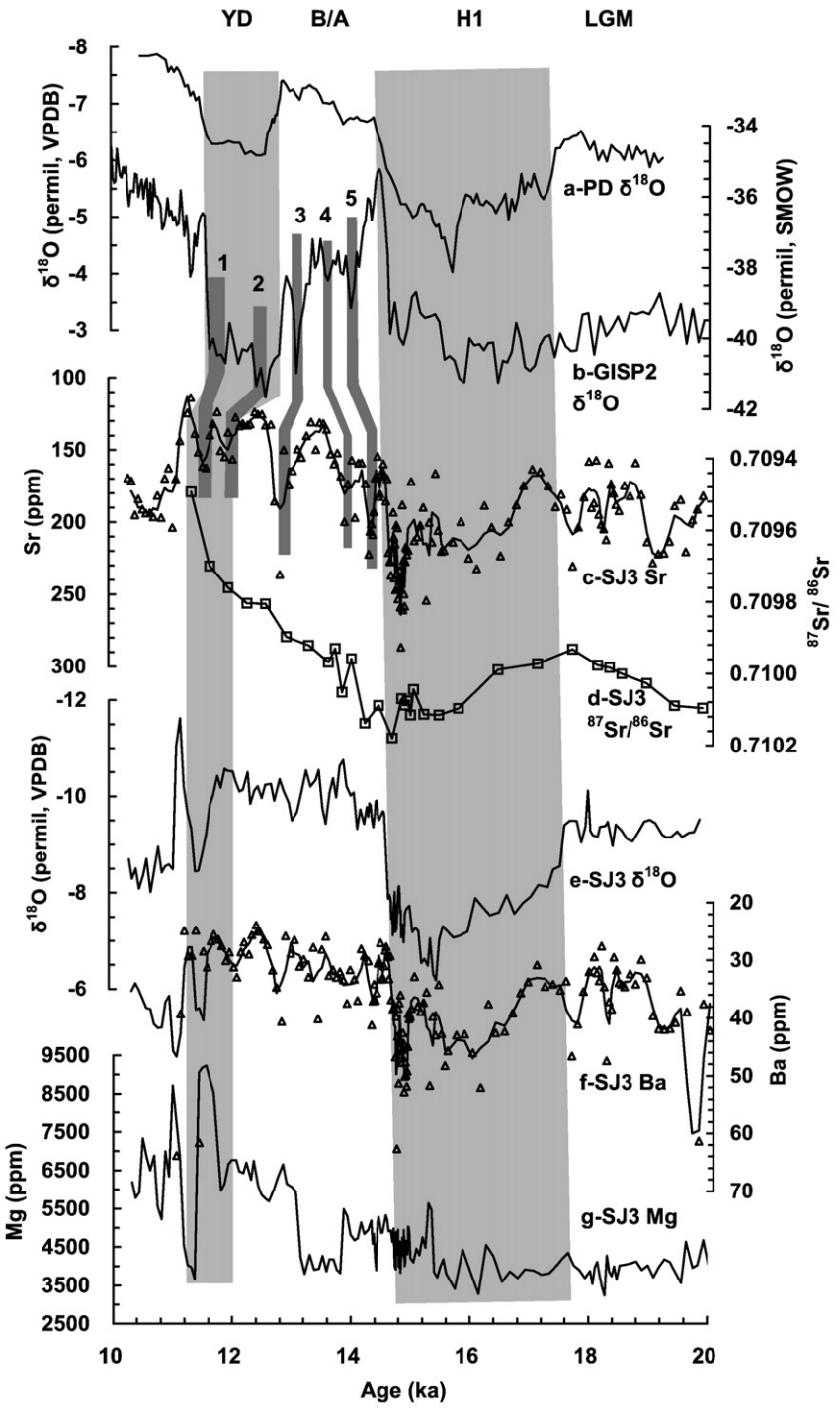

Fig. 8. Comparison of the Sr concentration (c) and $^{87}Sr/^{86}Sr$ ratio (d) variations of SJ3 with the speleothem $\delta^{18}O$ records of the same stalagmite (SJ3) (Zhou et al., 2008a) (e) and PD from Hulu cave in East China (Wang et al., 2001) (a), and the polar ice core $\delta^{18}O$ record (Grootes et al., 1993; Stuiver et al., 1995) (b). Also shown are the Ba (f) and Mg (g) records of SJ3. The solid line in (c), (f) and (g) represents a three-point running average trend of the data. The longer light grey bars indicate the two cold phases of the Younger Dyras and H1 events. The five shorter grey bars marked with 1–5 indicate small Sr peaks corresponding to five centennial cold events in the polar ice core during the B/A warm period and the YD cold reversal.

minerals. Previous investigations suggest that the carbonate fraction usually has a Sr concentration of > 1000 ppm, much higher than those of the silicate fraction of the aeolian sediments (~100 ppm, see Gallet et al., 1996 and Jahn et al., 2001) and marine carbonate rocks such as limestone (e.g. ~100–300 ppm in Nothdurft et al., 2004; Table 2). The following evidence suggests that the carbonate fraction, rather than all the minerals in the aeolian sediments is one of the main sources for Sr incorporated into SJ3. (1) The $^{87}Sr/^{86}Sr$ ratios of the leachate from the overlying soil layer is very close to the $^{87}Sr/^{86}Sr$ ratio of the carbonate fraction of the aeolian sediments in the top of the Luochuan loess-paleosol series (Yang et al., 2000); (2) Except two $^{87}Sr/^{86}Sr$ ratios in the top dirty part of SJ3, the $^{87}Sr/^{86}Sr$ ratio and the reciprocal of the Sr concentration (1/Sr) of SJ3 show a negative linear correlation ($r^2 = 0.75$) (Fig. 9), which suggests that the Sr sources for SJ3 may be dominated by mixing of two end-members, one more radiogenic with a higher Sr concentration and the other less radiogenic with a lower Sr concentration (Faure and Mensing, 2005). Extrapolating the linear $^{87}Sr/^{86}Sr$-1/Sr relationship to (1/Sr) = 0, we obtain a $^{87}Sr/^{86}Sr$ ratio of 0.7109, which is

Please cite this article as: Zhou, H., et al., Deglacial variations of Sr and $^{87}Sr/^{86}Sr$ ratio recorded by a stalagmite from Central China and their association with past climate and environment, Chemical Geology (2009), doi:10.1016/j.chemgeo.2009.09.003

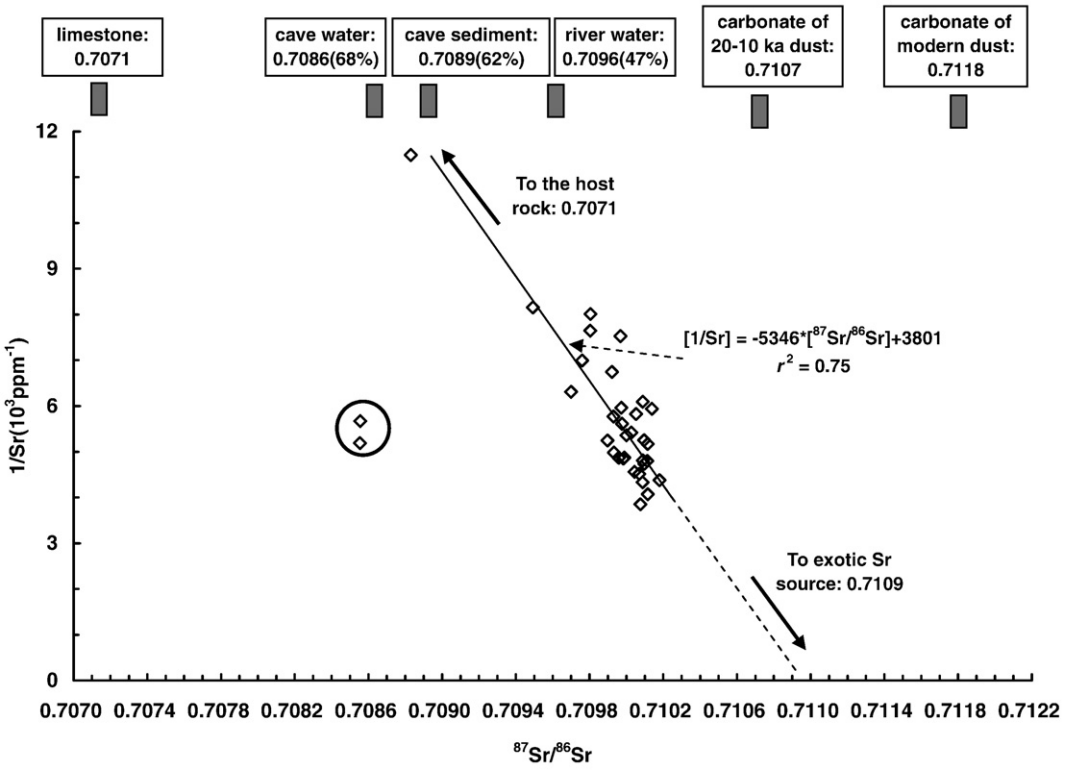

Fig. 9. The linear negative relationship between (1/Sr) and ($^{87}Sr/^{86}Sr$) for SJ3, reflecting two-component mixing, one component with lower Sr and $^{87}Sr/^{86}Sr$ (the Late Permian limestone), and the other with higher Sr and $^{87}Sr/^{86}Sr$ (the carbonate fraction of the aeolian sediments). The $^{87}Sr/^{86}Sr$ ratios of the two end-members, cave waters and sediments and river water are indicated above the 1/Sr–$^{87}Sr/^{86}Sr$ plot. The average $^{87}Sr/^{86}Sr$ ratio of 20–10 dust carbonate is from Yang et al. (2000). For waters and cave sediments, the percentages in parentheses indicate Sr proportion from the Late Permian limestone. The two data points in the circle are for samples from the top 6-mm section of the stalagmite, and deviate significantly from the 1/Sr–$^{87}Sr/^{86}Sr$ relationship defined by the rest of the data points. See text for discussion.

consistent with the $^{87}Sr/^{86}Sr$ value for the carbonate fraction in the 20–10 ka wind-blown dusts in the region (~0.7107 ± 0.0002, calculated using data from Yang et al., 2000). Although Sr from the silicate minerals in the aeolian sediments cannot be excluded completely, it should account only for a very small proportion because Sr released from silicate minerals under chemical weathering usually has a high $^{87}Sr/^{86}Sr$ ratio (Capo et al., 1998). For example, Jahn et al. (2001) and Gallet et al. (1996) estimated that the $^{87}Sr/^{86}Sr$ ratio of the silicate minerals in the loess-paleosol series in the Loess Plateau was between 0.720 and 0.725. Sun (2005) found that the fine fraction (<20 μm) of the silicate minerals in the aeolian sediments had $^{87}Sr/^{86}Sr$ ratios averaging 0.7246. If a mean $^{87}Sr/^{86}Sr$ ratio of 0.723 was assumed for the silicate minerals (Gallet et al., 1996; Jahn et al., 2001; Sun, 2005) and a $^{87}Sr/^{86}Sr$ ratio of 0.7116 was assumed for the modern carbonates (Yang et al., 2000) in the aeolian sediments, both our leaching experiments, whether by Milli-Q water or by 1% acetic acid, suggest that more than 95% of the Sr is released from the carbonate fraction of the aeolian sediments (Table 4).

The three bedrock samples give a mean $^{87}Sr/^{86}Sr$ ratio of 0.7071 (Table 4). If a mean $^{87}Sr/^{86}Sr$ ratio of 0.7118 is assumed for the leachates from the overlying soil layer, calculation using isotope mixing model (Faure and Mensing, 2005) indicates that on average ~70% of the Sr in the cave water was derived from the host rock while the remaining ~30% from the overlying soil layer (Fig. 9). As to the cave sediments, Sr leached by Milli-Q water gives a mean $^{87}Sr/^{86}Sr$ ratio of 0.7089 (Table 4), suggesting more than 60% of which deriving from the host rock (Fig. 9). Similarly, stalagmite SJ3 should derive its Sr from the two sources, the host rock and the carbonate fraction of the aeolian sediments. However, the latter had a $^{87}Sr/^{86}Sr$ ratio slightly lower than 0.7118 when SJ3 developed. The data from Yang et al. (2000) give a $^{87}Sr/^{86}Sr$ ratio of 0.7107 ± 0.0002 at 20–10 ka, consistent with the value deduced from the $^{87}Sr/^{86}Sr$-1/Sr relationship of SJ3 (Fig. 9). Because Luochuan is more than 400 km apart from the study site (Fig. 1) and the SJ3 $^{87}Sr/^{86}Sr$ record has a resolution twice better than the data of Yang et al. (2000) have, we assume 0.7109, the maximum value deduced from Fig. 9 for the exotic Sr source, for the carbonate fraction of aeolian sediments deposited at the study site at 20–10 ka. Except the top three points, the $^{87}Sr/^{86}Sr$ ratios of SJ3 suggest a Sr contribution of 19–37 % from the host rock, remarkably lower than the values for modern cave water (~70%) and leachates from cave sediments (>60%) (Fig. 9). This suggests that compared with cave sediments and modern cave water, stalagmite SJ3 developed at 20–10 ka during the last glacial has a much higher Sr contribution from the carbonate fraction of aeolian sediments.

5.3. Mechanisms controlling $^{87}Sr/^{86}Sr$ ratio variation

Variations in speleothem $^{87}Sr/^{86}Sr$ ratios reflect changes in relative contribution of various Sr sources of different $^{87}Sr/^{86}Sr$ ratios feeding the seepage water (Faure and Mensing, 2005), including the host rocks and one or more other Sr sources such as the overlying soil layer and atmospheric dust deposition (Banner et al., 1996; Goede et al., 1998; Ayalon et al., 1999; Bar-Matthews et al., 1999; Verheyden et al., 2000; Frumkin and Stein, 2004; Li et al., 2005a). For example, Banner et al. (1996) attributed the $^{87}Sr/^{86}Sr$ variation of several speleothems from Harrisons Cave on the island of Barbados to changes in groundwater compositions that, in turn, were a function of rainfall recharge in the area and interaction with bedrock. Goede et al. (1998) found that both Sr concentrations and $^{87}Sr/^{86}Sr$ ratios of a stalagmite from Frankcombe Cave in Tasmania (Australia) decreased significantly since ~70 ka and argued that higher Sr concentrations and $^{87}Sr/^{86}Sr$ ratios prior to ~70 ka were related to wind-blown ^{87}Sr-enriched dusts derived from the King Island region of what is now part of Bass Strait. In the EASM regime, Li et al. (2005a) attributed the $^{87}Sr/^{86}Sr$ variation

Please cite this article as: Zhou, H., et al., Deglacial variations of Sr and $^{87}Sr/^{86}Sr$ ratio recorded by a stalagmite from Central China and their association with past climate and environment, Chemical Geology (2009), doi:10.1016/j.chemgeo.2009.09.003

of stalagmite SFL from central China to changes in the provenance and the extent of chemical weathering of the epikarstic sediments, which were controlled by variations of paleo-summer monsoon.

Because the two Sr sources for SJ3 (the host rock and the carbonate fraction of aeolian sediments) have distinct $^{87}Sr/^{86}Sr$ ratios (Table 4 and see Section 5.2), their relative contribution would determine the variation of the $^{87}Sr/^{86}Sr$ ratio of SJ3. Although the $^{87}Sr/^{86}Sr$ ratios in the calcite fraction of the aeolian sediments deposited at Luochuan vary from 07104 to 0.7118 during the last glacial-interglacial cycle, their variation during marine isotope stage 2 was generally limited to 0.7105–0.7109 (Yang et al., 2000) and such variation alone could not account for either the large range or the trend of the $^{87}Sr/^{86}Sr$ values observed in SJ3 (Figs. 6d and 8d). The host rock is much less radiogenic compared with the leachate from the overlying soil layer (Table 4). An increase in Sr input from wind-blown dusts, or a reduction in Sr input from the host rock, or a combination of the two effects would result in an increase in the $^{87}Sr/^{86}Sr$ ratio of SJ3. Assuming that on average, the two Sr sources for SJ3 have $^{87}Sr/^{86}Sr$ ratios of 0.7109 and 0.7071, respectively, the Sr input from each source is calculated and illustrated in Fig. 10. Although there some small fluctuations, the Sr input from the host rock is relatively stable during 20–10 ka except the two sub-samples at growth hiatuses. The Sr input from wind-blown dust, however, displays remarkable variation. Especially during the H1 cold phase, the Sr input from wind-blown dust increased significantly (Fig. 10). These observations suggest that changes in Sr input from wind-blown dust dominate $^{87}Sr/^{86}Sr$ variation in SJ3.

5.4. Factors influencing Sr variation

Compared with the $^{87}Sr/^{86}Sr$ ratio, Sr in SJ3 is affected by much more complicated processes. For examples, there would be selective leaching of Sr from limestone (Fairchild et al., 2000) and fractionation of Sr would happen during precipitation of carbonate because the distribution coefficient of Sr between solution and carbonate (D_{Sr}) is significantly lower than unity (Veizer, 1983 and references therein). In general, Sr in speleothems was considered to be controlled by hydrological mixing in the epikarstic zone and vadose-zone dissolution-precipitation processes (Roberts et al., 1998, 1999; Fairchild et al., 2000, 2001; Huang et al., 2001). On annual scale, Fairchild et al. (2006a) had suggested three basic idealized patterns to interpret variations of trace element in speleothems, the fluid-dominated pattern, the crystal-dominated pattern and the temperature-controlled pattern. The fluid-dominated pattern primarily reflects changes in trace element concentration, or ratio of trace element to Ca^{2+} or CO_3^{2-} in the dripwater. For example, covariation of Sr and Mg resulted from prior calcite precipitation (PCP) (Fairchild et al., 2000; McMillan et al., 2005; Johnson et al., 2006) and significant increases in Sr and Mg at low flows (Baker et al., 2000; Fairchild et al., 2006b) are two typical cases of this pattern. The crystal-dominated pattern refers to the dominance of crystallographic factors in controlling trace element incorporation. A change in supersaturation state, or the presence of impurities, could lead to a change in crystal morphology and availability of surface sites at which trace species can be adsorbed and incorporated into the growing crystal. Mineralogy is also an important factor influencing Sr incorporation because D_{Sr} of aragonite is about 7–9 times greater than that of calcite (Veizer, 1983; Haskell et al., 1996 and references therein). Annual alternation of calcite and aragonite was previously reported in a stalagmite from Botswana (Railsback et al., 1994). The temperature-controlled pattern is the expected situation where significant temperature changes occur during the year since the Mg partition coefficient is temperature-dependent (Katz, 1973; Huang and Fairchild, 2001). More generally, as suggested by Fairchild et al. (2006a), the behaviour of trace elements can be influenced by different proportions of the three effects than is the case on the annual time-scale. For example, Treble et al. (2003), Finch et al. (2003) and Cruz et al. (2007) provide examples of elemental trends that reflect decadal and longer trends in rainfall, which differ in part from the behaviour of elements on the subannual scale.

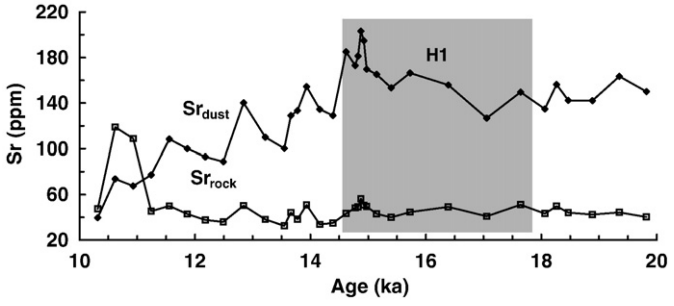

Fig. 10. Input of Sr in SJ3 from the host rock (Sr_{rock}) and wind-blown dust (Sr_{rock}). The grey bar indicates the coldest climatic phase (H1) since the LGM which is clearly presented in speleothem $\delta^{18}O$ records from the EASM regime (Wang et al., 2001; Zhou et al., 2008a).

The temperature effects on D_{Sr} determined by Katz et al. (1972) and Malone and Baker (1999) are too small to explain large variation of Sr in SJ3 (Figs. 6a and 8c), especially considering the fact that temperature variation in China since the Last Glacial Maximum (LGM) is usually less than 15 °C (Liu et al., 2002b) and that temperature in karstic cave is more stable than outside the cave. More importantly, higher Sr concentration occurs in colder phase such as H1 in SJ3 (Fig. 8c). This is opposite to the temperature effects on D_{Sr}. SJ3 is composed only of calcite and therefore, the influence of changing carbonate mineralogy on Sr concentration in SJ3 can be excluded. Impurity-related change in crystal morphology should not be responsible for the Sr increase during the H1 cold phase because Mn in SJ3, which could be regarded as an indicator of impurity, does not display significant change associated with the transition from the LGM to H1 (see Fig. 2 in Zhou et al., 2008c). Thus we suggest that the dominant controller of the long-term Sr trend of SJ3 should be the fluid, i.e. the chemical composition of groundwater seeping into Songjia Cave.

While studying the chemical composition of cave waters from Clamouse and Ernesto, Fairchild et al. (2000) suggested that there were four controlling mechanisms, (1) differential dissolution of calcite and dolomite in the host rocks, (2) PCP along flow paths, (3) incongruent dolomite dissolution, and (4) selective leaching of Mg and Sr with respect to Ca. As to SJ3, although CO_2 degassing and PCP along flow paths cannot be excluded and most probably occurs, however, they should not be the dominant factors responsible for the Sr variation because they usually results in co-variation of Sr/Ca and Mg/Ca (Fairchild et al., 2000; Johnson et al., 2006), which is not observed in SJ3 (Fig. 7A). All the distribution coefficients of Mg, Sr and Ba in carbonates are usually much smaller than unity (Veizer, 1983). A positive correlation between Mg and Sr or Ba would aid to be explained with significant CO_2 degassing. Although in addition to limestone, there are also some flint- and dolomite-limestone in the country rock at the study site (Zhou et al., 2008a), differential dissolution of the host rock would lead to higher Mg during cold-dry periods if it made a significant contribution to trace element variation (Fairchild et al., 2000). This is not observed in SJ3 (Fig. 8g). Like the PCP mechanism, selective leaching cannot explain either the totally different trends of Mg and Sr (Fig. 6a–b).

Long-term variations in Sr in speleothems may reflect not only palaeohydrology, but also changing source materials (Fairchild et al., 2000). We suggest that the most probable mechanism responsible for the long-term variation of Sr in SJ3 may be change of the relative contribution of the two Sr sources, the host rock and the overlying dust-derived soil layer. In addition to higher $^{87}Sr/^{86}Sr$ ratio, the carbonate fraction of wind-blown dust in Central China was expected

Please cite this article as: Zhou, H., et al., Deglacial variations of Sr and $^{87}Sr/^{86}Sr$ ratio recorded by a stalagmite from Central China and their association with past climate and environment, Chemical Geology (2009), doi:10.1016/j.chemgeo.2009.09.003

to have a Sr concentration of >1000 ppm (Gallet, et al., 1996; Jahn et al., 2001), significantly higher than the Sr concentration of the host rock (Table 2). Because atmospheric dust activity was intensive during the LGM and H1 cold phases and weakened since the last deglaciation (Xiao et al., 1995; Porter, 2001), its Sr export to SJ3 would be higher during the two cold phases and reduce progressively thereafter. With regard to Sr input from the host rock, on one hand, increased precipitation and decreased pH value of groundwater due to enhanced bio-activity and decomposition of organic matter under warm-humid climate should aid to dissolve more limestone. On the other hand, increased precipitation would strengthen the hydrological dynamics of the karstic groundwater and, in turn, reduce its residence time in aquifers and interaction with the host rock (Banner et al., 1996). It is not clear which effect is dominant when climate phase shifts. Thus change in Sr input from the host rock is determined by an integration of the two effects. The data illustrated in Fig. 10 suggest that the Sr input from the host rock is relatively stable, suggesting that the two opposite effects are comparable when SJ3 developed. Therefore, change in wind-blown dust is the dominant controller of Sr variations in SJ3.

5.5. A linkage of SJ3 Sr indices to the Asian winter monsoon

Both Sr and $^{87}Sr/^{86}Sr$ ratio of SJ3 are demonstrated to be controlled mainly by atmospheric dust activity. In East Asia, dust activity is thought to be an indicator of winter monsoon (Xiao et al., 1995; Porter, 2001) and some parameters of wind-blown dust such as grain size (Liu and Ding, 1998; Xiong et al., 2003) and flux (Xiao et al., 1995; Porter, 2001) are used as winter monsoon proxies. Greater grain size and higher flux indicate stronger winter monsoon. In Fig. 11 the Sr and $^{87}Sr/^{86}Sr$ ratio of SJ3 were tentatively compared with two winter monsoon records, the dust flux (Porter, 2001) and quartz median diameter (Q_{md}) (Xiao et al., 1995) reconstructed from the Luochuan loess profile (Fig. 1). Although the two winter monsoon records have much lower resolution (Xiao et al., 1995; Porter, 2001), their general trends are parallel to the Sr and $^{87}Sr/^{86}Sr$ ratio of SJ3 (Fig. 11a–e). This suggests a potential linkage between the SJ3 Sr geochemistry and the Asian winter monsoon. Enhanced winter monsoon indicated by greater flux and grain size under cold-dry climate (Xiao et al., 1995; Porter, 2001) has caused strengthened atmospheric dust activity and deposited more dust-derived carbonates, leading to higher Sr and $^{87}Sr/^{86}Sr$ ratio in SJ3.

6. Conclusion remarks

A long-term high-resolution Sr concentration profile coupled with a lower resolution $^{87}Sr/^{86}Sr$ record for stalagmite SJ3 from Sichuan province in Central China, which cover the last deglacial period, are shown to be closely associated with changes in past climate and environment, with higher Sr and more radiogenic $^{87}Sr/^{86}Sr$ ratio of SJ3 corresponding to cold climatic phases and vice versa. Atmospheric dust activity in this region is demonstrated to dominate variations of the two Sr indices, and a potential mechanism is suggested to link the SJ3 Sr geochemistry and Asian monsoon variations. Enhanced atmospheric dust activity associated with strengthened winter monsoon under cold climatic phases causes more dust-derived carbonates deposited at the study site and results in higher Sr and more radiogenic $^{87}Sr/^{86}Sr$ ratio recorded in SJ3. This study suggests

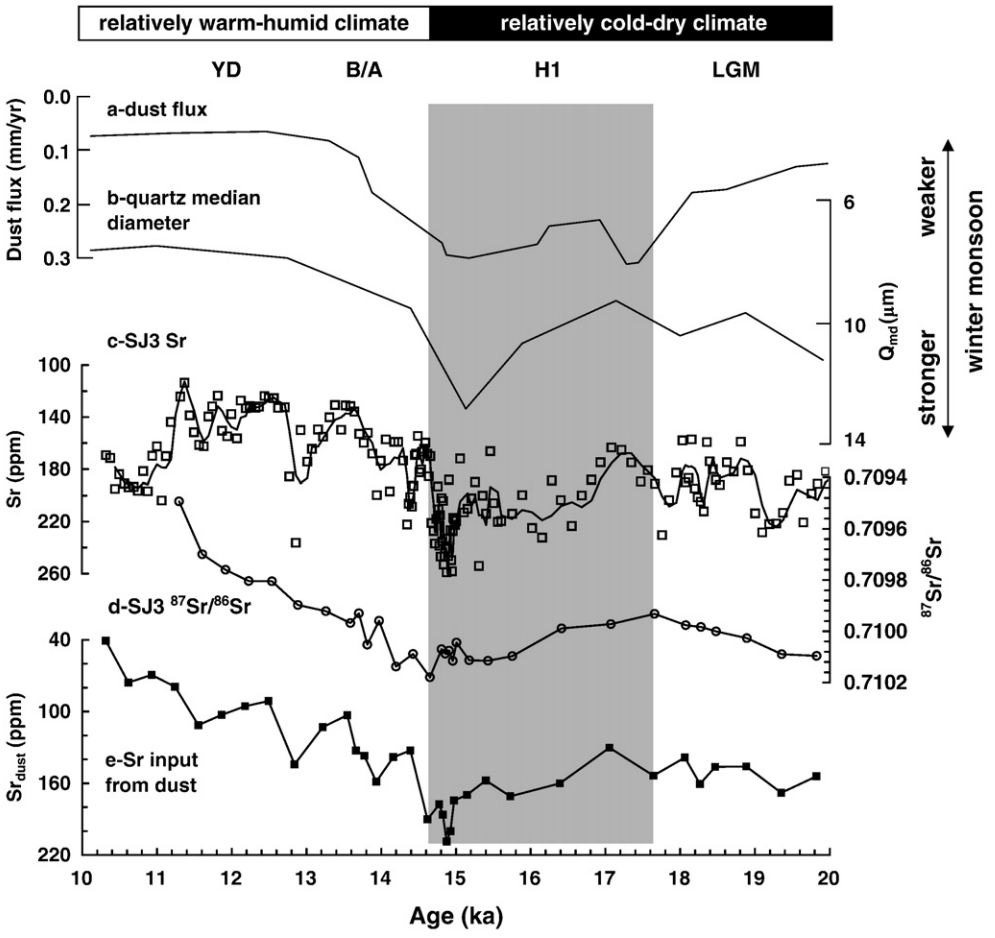

Fig. 11. Comparison of Sr concentrations (c), $^{87}Sr/^{86}Sr$ ratios (d) of SJ3 and calculated Sr input from wind-blown dust (e) with dust flux from Xiaheimu section, Luochuan (Porter, 2001) (a) and quartz median diameter (Q_{md}) from Luochuan section (Xiao et al., 1995). The solid line in (c) indicates the five-point running average trend of the data.

Please cite this article as: Zhou, H., et al., Deglacial variations of Sr and $^{87}Sr/^{86}Sr$ ratio recorded by a stalagmite from Central China and their association with past climate and environment, Chemical Geology (2009), doi:10.1016/j.chemgeo.2009.09.003

the possibility to use speleothems at the study site to reconstruct atmospheric dust activity and the Asian winter monsoon, which cannot be derived from conventionally used speleothem $\delta^{18}O$ and $\delta^{13}C$ records in the EASM regime. Especially, it suggests that speleothems developed at northeastern Sichuan Province have the potential to investigate the variability of atmospheric dust activity in East Asia on shorter time scales (such as centennial- to decadal-scale) because speleothems could be dated precisely (Edwards et al., 1987; Musgrove et al., 2001) and sampled at high spatial resolution. This seems impossible for dust-based researches due to dating limitation of the loess sediments and sampling resolution.

Although Sr concentration and $^{87}Sr/^{86}Sr$ ratio of speleothems have been suggested to be related with atmospheric dust activity in other areas (Goede et al., 1998; Ayalon et al., 1999; Bar-Matthews et al., 1999; Verheyden et al., 2000; Frumkin and Stein, 2004), this is the first attempt to correlate the speleothem-derived Sr and $^{87}Sr/^{86}Sr$ records with atmospheric dust activity and winter monsoon evolution in East Asia. However, this correlation needs to be corroborated with more examples and confirmed by replication test. Especially, monitoring seasonal variations of Sr and $^{87}Sr/^{86}Sr$ and annual flux of Sr at the study site would provide us some critical information for our explanation. Despite of these, the work presented here has far-reaching implications and may open a new window for the investigation of the Asian winter monsoon in the future.

Acknowledgements

We thank the chief editor (BB), Dr. Derek Vance and an anonymous reviewer for their thorough reviews and helpful comments on early versions of this paper. The research is financially supported by the project of NNSFC (40672120), the Key project of Guangdong natural science foundation (9251064004000001), the pilot project of Guangzhou Institute of Geochemistry (GIGCX-08-04) and the State Key Laboratory of Loess and Quaternary Geology (No. SKLLQG0815, SKLLQG0408). ^{230}Th dating at the HISPEC was supported by the NSC grants (94-2116-M-002-012; 95&96-2752-M002-012-PAE, and 97-2745-M-002-009 to CCS).Thanks are also due to Mr. Huang Jie and Wu Zheng for their help in sample collection, to Ms. Irina Kinaev for her help with Sr column chemistry at the University of Queensland, to Mr. Bo-Shian Wang, Chuan-Hsiung Chung and Ms. Tsai-Luen Yu for their help in $^{87}Sr/^{86}Sr$ determination at the EDSRC of NCKU, and to Ms. Liu Yin and Mr. Deng Wenfeng for their help in trace element analysis at Guangzhou Institute of Geochemistry.

References

Ayalon, A., Bar-Matthews, M., Kaufman, A., 1999. Petrography, strontium, barium and uranium concentrations, and strontium and uranium isotope ratios in speleothems as palaeoclimatic proxies: Soreq Cave, Israel. Holocene 9, 715–722.

Baker, A., Genty, D., Fairchild, I.J., 2000. Hydrological characterisation of stalagmite drip waters at Grotte de Villars, Dordogne, by the analysis of inorganic species and luminescent organic matter. Hydrology and Earth System Sciences 4, 439–449.

Baldini, J.U.L., McDermott, F., Fairchild, I.J., 2002. Structure of the 8200 year cold event revealed by a speleothem trace element record. Science 296, 2203–2206.

Banner, J.L., Musgrove, M., Asmerom, Y., Edwards, R.L., Hoff, J.A., 1996. High-resolution temporal record of Holocene ground-water chemistry: tracing links between climate and hydrology. Geology 24, 1049–1052.

Bar-Matthews, M., Ayalon, A., Kaufman, A., Wasserburg, G.J., 1999. The Eastern Mediterranean paleoclimate as a reflection of regional events: Soreq Cave, Israel. Earth and Planetary Science Letters 166, 85–95.

Bureau of Geology and Mineral Resources of Sichuan Province, 1991. Regional geology of Sichuan Province. Geological Publishing House, Beijing.

Burke, W.H., Denison, R.E., Hetherington, E.A., Koepnick, R.B., Nelson, H.F., Otto, J.B., 1982. Variation of seawater $^{87}SR/^{86}Sr$ throughout Phanerozoic time. Geology 10, 516–519.

Capo, R.C., Stewart, B.W., Chadwick, O.A., 1998. Strontium isotopes as tracers of ecosystem processes: theory and methods. Geoderma 82, 197–225.

Cheng, H., Edwards, R.L., Hoff, J., Gallup, C.D., Richards, D.A., Asmerom, Y., 2000. The half-lives of uranium-234 and thorium-230. Chemical Geology 169, 17–33.

Cruz Jr., F.W., Burns, S.J., Jercinovic, M., Karmann, I., Sharp, W.D., Vuille, M., 2007. Evidence of rainfall variations in Southern Brazil from trace element ratios (Mg/Ca and Sr/Ca) in a Late Pleistocene stalagmite. Geochimica et Cosmochimica Acta 71, 2250–2263.

Dykoski, C.A., Edwards, R.L., Cheng, H., Yuan, D., Cai, Y., Zhang, M., Lin, Y., Qing, J., An, Z., Revenauh, J., 2005. A high-resolution, absolute-dated Holocene and deglacial Asian monsoon record from Dongge Cave, China. Earth and Planetary Science Letters 233, 71–86.

Edwards, R.L., Chen, J.H., Wasserburg, G.J., 1987. ^{238}U–^{234}U–^{230}Th–^{232}Th systematics and the precise measurement of time over the past 500,000 years. Earth and Planetary Science Letters 81, 175–192.

Eggins, S.M., Woodhead, J.D., Kinsley, L.P.J., et al., 1997. A simple method for the precise determination of >40 trace elements in geological samples by ICPMS using enriched isotope internal standardisation. Chemical Geology 134, 311–326.

Fairchild, I.J., Borsato, A., Tooth, A.F., Frisia, S., Hawkesworth, C.J., Huang, Y., McDermott, F., Spiro, B., 2000. Controls on trace element (Sr–Mg) compositions of carbonate cave waters: implications for speleothem climatic records. Chemical Geology 166, 255–269.

Fairchild, I.J., Baker, A., Borsato, A., Frisia, S., Hinton, R.W., McDermott, F., Tooth, A.F., 2001. High-resolution, multiple trace-element variation in speleothems. Journal of Geological Society (London) 158, 831–841.

Fairchild, I.J., Smith, C.L., Baker, A., Fuller, L., Spötl, C., Mattey, D., McDermott, F., E.I.M.F., 2006a. Modification and preservation of environmental signals in speleothems. Earth-Science Reviews 75, 105–153.

Fairchild, I.J., Tuckwell, G.W., Baker, A., Tooth, A.F., 2006b. Modelling of dripwater hydrology and hydrogeochemistry in a weakly karstified aquifer (Bath, UK): implications for climate change studies. Journal of Hydrology 321, 213–231.

Fang, X.M., Li, J.J., Van der Voo, R., 1999. Age and provenance of loess in West Qinling. Chinese Science Bulletin 44 (23), 2188–2192.

Faure, G., Mensing, T.M., 2005. Isotopes: Principles and Applications, 3rd edition. John Wiley & Sons, pp. 347–362.

Finch, A.A., Shaw, P.A., Weedon, G.P., Holmgren, K., 2001. Trace element variation in speleothem aragonite: potential for palaeoenvironmental reconstruction. Earth and Planetary Science Letters 186, 255–267.

Finch, A.A., Shaw, P.A., Holmgren, K., Lee-Thorp, J., 2003. Corroborated rainfall records from aragonitic stalagmites. Earth and Planetary Science Letters 215, 265–273.

Frohlich, C., Hornbach, M.J., Taylor, F.W., Shen, C.-C., Moala, A., Morton, A.E., Kruger, J., 2009. Huge erratic boulders in Tonga deposited by a prehistoric tsunami. Geology 37, 131–134.

Frumkin, A., Stein, M., 2004. The Sahara–East Mediterranean dust and climate connection revealed by strontium and uranium isotopes in a Jerusalem speleothem. Earth and Planetary Science Letters 217, 451–464.

Gallet, S., Jahn, B.M., Torii, M., 1996. Geochemical characterization of loess-paleosol sequence from the Luochuan section, China and its paleoclimatic implications. Chemical Geology 133, 67–88.

Ginoux, P., Chin, M., Tegen, I., Prospero, J.M., Holben, B., Dubvoik, O., Lin, S.-J., 2001. Sources and distributions of dust aerosols simulated with the GOCART model. Journal of Geophysical Research 106, 20255–20273.

Goede, A., McCulloch, M., McDermott, F., Hawkesworth, C., 1998. Aeolian contribution to strontium and strontium isotope variations in a Tasmanian speleothem. Chemical Geology 149, 37–50.

Grootes, P.M., Stuiver, M., White, J.W.C., Johnsen, S., Jouzel, J.J., 1993. Comparison of oxygen isotope records from the GISP2 and GRIP Greenland ice cores. Nature 366, 552–554.

Haskell, B.J., Engstrom, D.R., Fritz, S.C., 1996. Late Quaternary paleohydrology in the North American Great Plains inferred from the geochemistry of endogenic carbonate and fossil ostracodes from Devils Lake, North Dakota, USA. Palaeogeography, Palaeoclimatology, Palaeoecology 124, 179–193.

Hellstrom, J.C., McCulloch, M.T., 2000. Multi-proxy constraints on the climatic significance of trace element records from a New Zealand speleothem. Earth and Planetary Science Letters 179, 287–297.

Hodell, D.A., 1994. Progress and paradox in strontium isotope stratigraphy. Paleoceanography 9, 395–398.

Hu, C.Y., Huang, J.H., Fang, N.Q., Xie, S.C., Henderson, G.M., Cai, Y.J., 2005. Adsorbed silica in stalagmite carbonate and its relationship to past rainfall. Geochimica et Cosmochimica Acta 69, 2285–2292.

Hu, C.Y., Henderson, G.M., Huang, J.H., Xie, S., Sun, Y., Johnson, K.R., 2008. Quantification of Holocene Asian monsoon rainfall from spatially separated cave records. Earth and Planetary Science Letters 266 (3–4), 221–232.

Huang, Y., Fairchild, I.J., 2001. Partitioning of Sr^{2+} and Mg^{2+} into calcite under karst-analogue experimental conditions. Geochimica et Cosmochimica Acta 65, 47–62.

Huang, Y., Fairchild, I.J., Borsato, A., Frisia, S., Cassidy, N.J., McDermott, F., Hawkesworth, C.J., 2001. Seasonal variations in Sr, Mg and P in modern speleothems (Grotta di Ernesto, Italy). Chemical Geology 175, 429–448.

Jaffey, A.H., Flynn, K.F., Glendenin, L.E., Bentley, W.C., Essling, A.M., 1971. Precision measurement of half-lives and specific activities of ^{235}U and ^{238}U. Physical Reviews C 4, 1889–1906.

Jahn, B.M., Gallet, S., Han, J.M., 2001. Geochemistry of the Xining, Xifeng and Jixian sections, Loess Plateau of China: Eolian dust provenance and paleosol evolution during the last 140 ka. Chemical Geology 178, 71–94.

Johnson, K.R., Hu, C., Belshaw, N.S., Henderson, G.M., 2006. Seasonal trace-element and stable-isotope variations in a Chinese speleothem: the potential for high-resolution paleomonsoon reconstruction. Earth and Planetary Science Letters 244, 394–407.

Katz, A., 1973. The interaction of magnesium with calcite during crystal growth at 25–90 °C and one atmosphere. Geochimica et Cosmochimica Acta 37, 1563–1586.

Katz, A., Starinsky, S.E., Holland, H.D., 1972. Strontium behavior in the aragonite–calcite transformation: an experimental study at 40–98 °C. Geochimica et Cosmochimica Acta 36, 481–496.

Please cite this article as: Zhou, H., et al., Deglacial variations of Sr and $^{87}Sr/^{86}Sr$ ratio recorded by a stalagmite from Central China and their association with past climate and environment, Chemical Geology (2009), doi:10.1016/j.chemgeo.2009.09.003

Lei, X.Y., Yue, L.P., Wang, J.Q., Zhang, L., 1998. Magnetic characteristics and their paleoclimatic significance of Fengzhou loess in the Qinling Mountains of China. Chinese Science Bulletin 43, 1571–1575.
Li, H.-C., Ku, T.-L., You, C.-F., Cheng, H., Edwards, R.L., Ma, Z.B., Tsai, W.S., Li, M.D., 2005a. $^{87}Sr/^{86}Sr$ and Sr/Ca in speleothems for paleoclimate reconstruction in Central China between 70 and 280 kyr ago. Geochimica et Cosmochimica Acta 69, 3933–3947.
Li, B.P., Greig, A., Zhao, J.X., Collerson, K.D., Quan, K.S., Meng, Y.H., Ma, Z.L., 2005b. ICP-MS trace element analysis of Song dynasty porcelains from Ding, Jiexiu and Guantai kilns, north China. Journal of Archaeological Science 32 (2), 251–259.
Liu, T.S. (Ed.), 1985. Loess and Environment. China Ocean Press, Beijing, pp. 1–234.
Liu, T.S., Ding, Z.L., 1998. Chinese loess and the paleomonsoon. Annual Review of Earth and Planetary Sciences 26, 111–145.
Liu, L.W., Chen, J., Chen, Y., Ji, J.F., 2002a. Sequential extraction procedure of loess and paleosol and the implications of Rb/Sr ratios. Acta Pedologica Sinica 39, 65–70 (In Chinese with English abstract).
Liu, J., Yu, G., Chen, X., 2002b. Palaeoclimate simulation of 21 ka for the Tibetan Plateau and Eastern Asia. Climate Dynamics 19, 575–583.
Ma, Z.B., Li, H.C., Xia, M., Ku, T.L., Peng, Z.C., Chen, Y.S., Zhang, Z.F., 2003. Paleotemperature changes over the past 3000 years in eastern Beijing, China: a reconstruction based on Mg/Sr records in a stalagmite. Chinese Science Bulletin 48 (4), 395–400.
Malone, M.J., Baker, P.A., 1999. Temperature dependence of the strontium distribution coefficient in calcite: an experimental study from 40 to 200 C and application to natural diagnetic calcites. Journal of Sedimentary Reseach 69, 216–233.
McMillan, E., Fairchild, I.J., Frisia, S., Borsato, A., McDermott, F., 2005. Annual trace element cycles in calcite–aragonite speleothems: evidence of drought in the western Mediterranean 1200–1100 yr BP. Journal of Quaternary Science 20, 423–433.
Musgrove, M., Banner, J.L., Mack, L.E., Combs, D.M., James, E.W., Cheng, H., Edwards, R.L., 2001. Geochronology of late Pleistocene to Holocene speleothems from Central Texas: implications for regional paleoclimate. Geological Society of America Bulletin 113, 1532–1543.
Nakano, T., Tazawa, K., Na, C., Tase, N., Itoda, N., Kaneshima, H., 1993. Sr isotopic composition of stalactite in the cave of Gyokusendo, Okinawa. Annual Report of the Institute of Geoscience, vol. 19. University of Tsukuba, pp. 79–82.
Nothdurft, L.D., Webb, G.E., Kamber, B.S., 2004. Rare earth element geochemistry of Late Devonian reefal carbonates, canning basin, Western Australia: confirmation of a seawater REE proxy in ancient limestones. Geochimica et Cosmochimica Acta 68 (2), 263–283.
Porter, S.C., 2001. Chinese loess record of monsoon climate during the last glacial-interglacial cycle. Earth-Science Reviews 54, 115–128.
Railsback, L.B., Brook, G.A., Chen, J., Kalin, R., Fleisher, C.J., 1994. Environmental controls on the petrology of a late Holocene speleothem from Botswana with annual layers of aragonite and calcite. Journal of Sedimentary Research 64, 147–155.
Ren, J.Z., Ding, Z.L., Liu, T.S., Sun, J.M., Zhou, X.Q., 1996. Climatic changes on millennial time scales — evidence from a high-resolution loess record. Science in China (Series D) 39, 449–459.
Richter, D.K., Götte, T., Niggemann, S., Wurth, G., 2004. REE^{3+} and Mn^{2+} activated cathodoluminescence in lateglacial and Holocene stalagmites of central Europe: evidence for climatic processes? The Holocene 14, 759–767.
Roberts, M.S., Smart, P., Baker, A., 1998. Annual trace element variations in a Holocene speleothem. Earth and Planetary Science Letters 154, 237–246.
Roberts, M.S., Smart, P.L., Hawkesworth, C.J., Perkins, W.T., Pearce, N.J.G., 1999. Trace element variations in coeval Holocene speleothems from GB Cave, southwest England. The Holocene 9, 707–713.
Shen, C.-C., Edwards, R.L., Cheng, H., Dorale, J.A., Thomas, R.B., Moran, S.B., Weinstein, S.E., Edmonds, H.N., 2002. Uranium and thorium isotopic and concentration measurements by magnetic sector inductively coupled plasma mass spectrometry. Chemical Geology 185, 165–178.
Sinomaps Press, 1984. Atlas of the People's Republic of China. Sinomaps Press, Beijing.
Stirling, C.H., Andersen, M.B., Potter, E.-K., Halliday, A.N., 2007. Low temperature isotope fractionation of uranium. Earth and Planetary Science Letters 264, 208–225.
Stuiver, M., Grootes, P.M., Braziunas, T.F., 1995. The GISP2 delta 18O climate record of the past 16, 500 years and the role of the sun, ocean, and volcanoes. Quaternary Research 44, 341–354.
Sun, J.M., 2005. Nd and Sr isotopic variations in Chinese eolian deposits during the past 8 Ma: Implications for provenance change. Earth and Planetary Science Letters 240, 454–466.
Taylor, S.R., McLennan, S.M., 1985. The continental crust: its composition and evolution. Blackwell, Oxford.
Treble, P., Shelley, J.M.G., Chappell, J., 2003. High resolution subannual records of trace elements in a modern (1911–1992) speleothem from southwest Australia. Earth and Planetary Science Letters 216, 141–153.
Veizer, J., 1983. Chemical diafenesis of carbonates: theory and application of trace element technique. In: Arthur, M.A., et al. (Ed.), Stable isotopes in sedimentary geology, SEPM short course, vol. 10.
Verheyden, S., Keppens, E., Fairchild, I.J., McDermott, F., Weis, D., 2000. Mg, Sr and Sr isotope geochemistry of a Belgian Holocene speleothem: implications for paleoclimate reconstructions. Chemical Geology 169, 131–144.
Wang, Y.J., Cheng, H., Edwards, R.L., An, Z.S., Wu, J.Y., Shen, C.C., Dorale, J.A., 2001. A high-resolution absolute-dated late Pleistocene monsoon record from Hulu Cave, China. Science 294, 2345–2348.
Wang, Y.J., Cheng, H., Edwards, R.L., Kong, X.G., Shao, X.H., Chen, S.T., Wu, J.Y., Jiang, X.Y., Wang, X.F., An, Z.S., 2008. Millennial- and orbital-scale changes in the East Asian monsoon over the past 224, 000 years. Nature 451, 1090–1093.
Weyer, S., Anbar, A.D., Gerdes, A., Gordon, G.W., Algeo, T.J., Boyle, E.A., 2008. Natural fractionation of $^{238}U/^{235}U$. Geochimica et Cosmochimica Acta 72, 345–359.
Wen, Q.Z., et al., 1989. Geochemistry of the Chinese Loess. Chinese Science Press, Beijing. pp. 1–285.
Xiao, J.L., Porter, S.C., An, Z.S., Kumai, H., Yoshikawa, S., 1995. Grain size of quartz as an indicator of winter monsoon strength on the Loess Plateau of central China during the last 130000 yr. Quaternary Research 43, 22–29.
Xiong, S.F., Ding, Z.L., Jiang, W.Y., Yang, S.L., Liu, T.S., 2003. Damped fluctuations in Chinese loess grain size. Geophysical Research Letters 30 (19), 2007. doi:10.1029/2003GL018187.
Yang, J.D., Chen, J., An, Z.S., Shields, G., Tao, X.C., Zhu, H.B., Ji, J.F., Chen, Y., 2000. Variations in $^{87}Sr/^{86}Sr$ ratios of calcites in Chinese loess: a proxy for chemical weathering associated with the East Asian summer monsoon. Palaeogeography, Palaeoclimatology, Palaeoecology 157, 151–159.
Yuan, D.X., Cheng, H., Edwards, R.L., Dykoski, C.A., Kelly, M.J., Zhang, M.L., Qin, J.M., Lin, Y.S., Wang, Y.J., Wu, J.Y., Dorale, J.A., An, Z.S., Cai, Y.J., 2004. Timing, duration, and transitions of the Last Interglacial Asian Monsoon. Science 304, 575–578.
Zhao, J.X., Hu, K., Collerson, K.D., Xu, H.K., 2001. Thermal ionization mass spectrometry U-series dating of a hominid site near Nanjing, China. Geology 29, 27–30.
Zhao, J.X., Wang, Y.J., Collerson, K.D., Gagan, M.K., 2003. Speleothem U-series dating of semi-synchronous climate oscillations during the last deglaciation. Earth and Planetary Science Letters 216 (1–2), 155–161.
Zhou, H.Y., Li, T.G., Jia, G.D., Zhu, Z.Y., Chi, B.Q., Cao, Q.Y., Sun, R.T., Peng, P.A., 2007. Sea surface temperature reconstruction for the Middle Okinawa Trough during the last glacial-interglacial cycle using C37 unsaturated alkenones. Palaeogeography, Palaeoclimatology, Palaeoecology 246, 440–453.
Zhou, H.Y., Zhao, J.X., Feng, Y.X., Gagan, M.K., Zhou, G.Q., Yan, J., 2008a. Distinct climate change synchronous with Heinrich event one, recorded by stable oxygen and carbon isotopic compositions in stalagmites from China. Quaternary Research 69, 306–315.
Zhou, H.Y., Zhao, J.X., Zhang, P.Z., Shen, C.-C., Chi, B.Q., Feng, Y.X., Lin, Y., Guan, H.Z., You, C.-F., 2008b. Decoupling of stalagmite-derived Asian summer monsoon records from North Atlantic temperature change during marine oxygen isotope stage 5d. Quaternary Research 70, 315–321.
Zhou, H.Y., Chi, B.Q., Lawrence, M., Zhao, J.X., Yan, J., Greig, A., Feng, Y.X., 2008c. High resolution and precisely dated record of weathering and hydrological dynamics recorded by manganese and rare earth elements in a stalagmite from central China. Quaternary Research 69, 438–446.
Zhou, H.Y., Wang, Q., Zhao, J.X., Zheng, L.N., Guan, H.Z., Feng, Y.X., Greig, A., 2008d. Rare earth elements and yttrium in a stalagmite from Central China and potential paleoclimatic implications. Palaeogeography, Palaeoclimatology, Palaeoecology 270, 128–138.

Please cite this article as: Zhou, H., et al., Deglacial variations of Sr and $^{87}Sr/^{86}Sr$ ratio recorded by a stalagmite from Central China and their association with past climate and environment, Chemical Geology (2009), doi:10.1016/j.chemgeo.2009.09.003